NONEQUILIBRIUM ISOTOPE EFFECTS IN THE UNIMOLECULAR REACTIONS OF CHEMICALLY ACTIVATED CHLOROETHANES

by

KENNETH DEES

B. S., Utah State University, 1965

A MASTER'S THESIS

submitted in partial fulfillment of the

requirements for the degree

MASTER OF SCIENCE

Department of Chemistry

KANSAS STATE UNIVERSITY
Manhattan, Kansas

1968

Approved by:

D. W. Setser

Major Professor

TABLE OF CONTENTS

LIST OF TABLES

LIST OF FIGURES

INTRODUCTION

The main purpose of this work was to investigate the non-equilibrium, unimolecular kinetic isotope effects for HCl and DCl elimination from C_2H_5Cl and C_2D_5l and 1,2-$C_2H_4Cl_2$ and 1,2-$C_2D_4Cl_2$. The vibrationally excited molecules which were generated by the combination of methyl and chloromethyl radicals, are at an energy of ≈ 90 kcal mole^{-1}. These intermolecular kinetic isotope effects are a combination of primary and secondary types. The experimental results were interpreted on the basis of a four-centered transition state (1,2,3) using the quantum statistical theory of unimolecular reactions commonly called the RRKM theory (4,5,6). A second purpose of this work was to measure the collisional deactivation probabilities for these vibrationally excited molecules. Since the critical energy for the elimination reactions is about 55 kcal mole^{-1}, the energy region of interest spans from about 90 to a few kcal mole^{-1} above 55 kcal mole^{-1}. The collisional deactivation probabilities were measured by comparing the competition between unimolecular reaction and collisional deactivation at low pressures (7). It was of special interest to learn whether or not the deactivation probabilities exhibit an isotope effect; this work represents the first attempt to measure such effects.

The nonequilibrium rate constants for the HCl elimination reactions of chemically activated C_2H_5Cl and 1,2-$C_2H_4Cl_2$ have been previously reported from this laboratory (8,9) and also the

thermal pyrolysis studies of these compounds have been done by several investigators (10-16). The unusual nature of the four-centered transition state for HCl eliminations from C_2H_5Cl and 1,2-$C_2H_4Cl_2$ make it an especially interesting case for treatment by the RRKM theory. The experimental rate constants were successfully interpreted using a four-centered transition state (2) described by bond orders connecting the four centers, in conjunction with the RRKM theory. The applicability of this four-centered transition state was successfully extended to unimolecular elimination reactions of C_2H_5Br, 1,2-$C_2H_4Br_2$, and 1,2-C_2H_4BrCl (3). The isotope effect data obtained in this work represents an attempt to obtain a more critical test for the proposed transition state of these four-centered elimination reactions. Other isotope data from thermal activation studies are also useful for this purpose. Blades, et. al. (17) have reported on the thermal intramolecular isotope effect for Ethyl 1,1,2,2-d_4 chloride. Heydtmann and Volker (18) have reported on the thermal equilibrium fall-off data for C_2H_5Cl and C_2D_5Cl. Holbrook and Marsh (15) have reported on the fall-off region of C_2H_5Cl and compared the results to several unimolecular theories. No good thermal equilibrium or thermal fall-off data have been reported for $C_2H_4Cl_2$. All of these relevant data are included in the characterization of the four-centered elimination reactions. Rabinovitch and coworkers (19-26) have reported on the existence and measurement of large statistical isotope

effects in unimolecular decompositions of energized species. These workers and others (18,27) have demonstrated the applicability of the RRKM theory in explaining and predicting the isotope effect and that formulation is the basis of the treatment used here.

The collisional deactivation of 1,2-$C_2H_4Cl_2$ by several types of bath molecules (28) has recently been reported from this laboratory based upon a simple stepladder deactivation model (7); the average increment of energy transferred per gas kinetic collision was ≈ 12 kcal mole^{-1} for CH_3Cl, CH_2Cl_2, and CF_4 and ≈ 6 kcal mole^{-1} for N_2 and Ar. The observation was made that collisions between molecules each having permanent dipoles seem to have no special effect for the energy transfer probabilities. Other work on vibrational energy transfer in the low energy region is voluminous (29), vibrational-translational, vibrational-rotational, and vibrational-vibrational exchange have received study both experimentally and theoretically, however, quantitative data for polyatomic molecules at high energies are scarce (7). This work enables an estimate to be given of the vibrational energy transfer probabilities for C_2H_5Cl, C_2D_5Cl, and $C_2D_4Cl_2$ with CH_3Cl and CD_3Cl; the measurements of reference 28 were also verified for CH_3Cl with $C_2H_4Cl_2$. The accuracy of the present data are not high but in view of the critical lack of information about the role of vibrational energy in collisional processes involving large quantities of energy, these data are useful and support existing (9) trends in the literature.

This work owes explicit acknowledgement to the work of Dr. J. C. Hassler (1) on these four-centered reactions. Some of the previous calculations have been repeated in order to take advantage of improved models. The actual numerical values used in this thesis are the favored ones, but the method and spirit of approach are the same.

EXPERIMENTAL

Reagents. Chloromethane-h_3 was purchased from Matheson Company, Inc. and chloromethane-d_3 was purchased from Merck Sharp & Dohme of Canada Limited, Montreal, Canada. The original reagents were tested for chemical purity by gas-solid-phase-chromatography analysis and were found to be sufficiently pure so that further treatment was not necessary. Ketene-h_2 and ketene-d_2 were prepared by pyrolysis (wire heated to a barely red color) of acetone-h_6 and acetone-d_6 respectively. The acetone-d_6 was also purchased from Merck Sharp & Dohme of Canada Limited. The main impurities of the ketene were low boiling components that were removed by selective trap to trap distillation. The ketene was finally purified by gas-solid-phase-chromatography at -78 C on a 20-30 ft. Tygon column packed with Fluoropack. Mass spectrographic analysis of the ketene-d_2 was somewhat ambiguous. In principle the percentage of ketene-d_1 can be calculated by comparing the mass 43 peak to the mass 44 peak. If the work was done very rapidly the percentage of ketene-d_1 was 10%. However, upon standing in the inlet of the mass spectrometer, the percentage of ketene-d_1 increased with time probably by means of an exchange reaction in the entry chambers of the mass spectrometer. This same result occurred with two different mass spectrometers and two different operators. To insure that the ketene-d_2 was sufficiently pure, the products of the deuterated reactions were also analyzed for purity. The results indicated that the

products 1,2-dichloroethane-d_4, chloroethane-d_5, and ethane-d_6 had 8-10% h_1 isotopic impurity. The chloromethane-d_3, as indicated by direct mass spectrographic analysis was ≈ 99% deuterated.

Procedure. The general method consisted of photolyzing mixtures of chloromethane-h_3 and ketene-h_2 or chloromethane-d_3 and ketene-d_2 at room temperature in Pyrex vessels at various pressures. The methylene created from the photolysis of ketene undergoes reaction with the constituents of the gas sample. The products were analyzed by gas chromatography. The procedures are described in detail below.

Mixtures of chloromethane-h_3 and ketene-h_2 or chloromethane-d_3 and ketene-d_2 in the ratio of 5 to 10:1 were sealed into pyrex vessels ranging from .7 cc to 500 cc depending upon the desired pressure range. The samples were then photolyzed for approximately one hour. The light source was a General Electric AH-6 high pressure mercury arc. A solution filter of $NiSO_4$ and $CoSO_4$* was used to isolate the 3200 A light for ketene photolysis. Analysis of the photolyzed sample was done by gas-solid-phase-chromatography. The gas chromatography unit was a Perkin-Elmer 820 with a four filament differential hot wire thermal conductivity detector. Helium was used as the carrier gas. A short firebrick column 2-3 inches long was used in the inlet system to adsorb any unreacted ketene. A 16 ft. 1/4 inch diameter stainless steel column packed with Poropak S was used to separate the components. Quantitative calibration for each component

*The solution (30) was prepared as follows: 46 grams of $NiSO_4 \cdot 6H_2O$ and 14 grams of $CoSO_4 \cdot 7H_2O$ was dissolved in 100 grams H_2O.

were made by utilizing standard mixtures prepared to approximate the composition of actual photolyzed samples.

All sample preparation was done on a standard vacuum rack. Contact of the gases with stopcock grease was minimized in the following way: The gas burette used in measuring gas samples was equipped with greaseless valves (31) having Viton-A diaphragms. These valves did not absorb measureable quantities of chloroalkanes during the period of measurement. The samples, after photolysis, were cracked open into a gas-chromatography inlet system which contained only metal valves; the grease points consisted of only the standard taper joints. A standard mixture sample containing a known amount of products and reactants was used to test the inlet system. No measureable quantities were absorbed.

Analysis were made for the following principle components: vinyl chloride, ethyl chloride, ethane, and 1,2-dichloroethane; deuterated and non-deuterated compounds were found to have the same retention time and sensitivity. Four methods employing temperature programming were used to accomplish the analyses: Method 1. This method was developed in order to separate chloromethane, vinyl chloride, chloroethane, and 1,2-dichloroethane in one pass through the column; they are eluted in the above order. The temperature was initially 87-88 C and was programmed to approximately 135 C just after the chloroethane peak. The following technique gave a stable baseline; the column oven was heated to 150 C very quickly and then the temperature was

permitted to level-off to approximately 135 C before the 1,2-dichloroethane was eluted. Average retention times were as follows: chloromethane, 5 min. 40 sec.; vinyl chloride, 11 min. 30 sec.; chloroethane, 23 min.; 1,2-dichloroethane, 22-24 min. after temperature programming. The variance in the retention time of 1,2-dichloroethane did not appreciably alter the sensitivity (cc/ph, cubic centimeters/peak height). On the other hand, the chloroethane sensitivity proved to vary with both temperature and retention time and exactly reproducible conditions had to be maintained for each run.

Method 2. This method was developed primarily to measure ethane and 1,2-dichloroethane during the same run (see ethane analysis); the main difficulty is separating the ethane and ethene. The initial temperature was 27 C; the temperature was programmed to 135 C after 10 min. This, as in method 1, was done by heating the column oven to 150 C very quickly, then letting the temperature level-off to approximately 135 C before the 1,2-dichloreothane was eluted. Average retention times were as follows: Ethene, 6 min.; ethane, 8 min 30 sec; chloromethane, 14 min. 12 sec.; 1,2-dichloroethane, 44-46 min. (total time including temperature programming). Again small deviations in retention time for 1,2-dichloroethane did not affect the sensitivity to any great extent.

Method 3. This method was used for high pressure runs where the amount of vinyl chloride was negligible and only analysis for chloroethane and 1,2-dichloroethane were desired. No temperature programming was needed; the temperature was 126 C. The average retention times were as follows: Chloromethane, 2 min. 48 sec.; chloroethane, 7 min. 12 sec.; 1,2-dichloroethane, 42 min. 45 sec.

Method 4. Only a few of the early runs employed this method. The first three methods proved to be better because of the convenience and increased accuracy of a single pass analysis. For this method the photolyzed sample was first passed through a 12 ft. Octoil-S column at 100 C to obtain analysis for 1,2-dichloroethane. The light components were trapped from the effluent and run through the Poropak S column at 84 C to obtain analysis for vinyl chloride. The method was used only for studying 1,2-dichloroethane decomposition.

RESULTS

Reaction mechanism at high pressures. Earlier work (8,9) from this laboratory established the general features of the reaction between methylene and chloromethane. The equations which describe the main reactions at high pressure (≳100 cm) are

$$CH_2CO + h\nu \longrightarrow CH_2 + CO \qquad (1a)$$

$$CH_2 + CH_2CO \longrightarrow C_2H_4 + CO \qquad (1b)$$

$$CH_2 + CH_3Cl \xrightarrow{k_x} CH_3 + CH_2Cl \qquad (1c)$$

$$CH_3 + CH_3 \xrightarrow{k_1} C_2H_6 \qquad (1d)$$

$$CH_3 + CH_2Cl \xrightarrow{k_2} CH_3CH_2Cl \qquad (1e)$$

$$CH_2Cl + CH_2Cl \xrightarrow{k_3} ClCH_2CH_2Cl \qquad (1f)$$

An equivalent set exists for the deuterated system.

$$CD_2CO + h\nu \longrightarrow CD_2 + CO \qquad (1a')$$

$$CD_2 + CD_2CO \longrightarrow C_2D_4 + CO \qquad (1b')$$

$$CD_2 + CD_3Cl \xrightarrow{k_x'} CD_3 + CD_2Cl \qquad (1c')$$

$$CD_3 + CD_3 \xrightarrow{k_1'} C_2D_6 \qquad (1d')$$

$$CD_3 + CD_2Cl \xrightarrow{k_2'} CD_3CD_2Cl \qquad (1e')$$

$$CD_2 + CD_2Cl \xrightarrow{k_3'} ClCD_2CD_2Cl \qquad (1f')$$

Ethane and 1,2-dichloroethane can only be explained by a chlorine or hydrogen abstraction mechanism; CH_2 insertion reactions are

thus not important. The combined rate constant for H and Cl abstraction from CH_3Cl is k_x. Ethene is formed by the attack of CH_2 upon ketene. As will be discussed later, this leads to some difficulties in determining the chloroethane decomposition rate constant because ethene is also a product of this decomposition reaction.

Secondary radical reactions that could be expected are

$$CH_3 + CH_3Cl \longrightarrow CH_4 + CH_2Cl \qquad (2a)$$

$$CH_2Cl + CH_3Cl \longrightarrow CH_2Cl_2 + CH_3 \qquad (2b)$$

Equivalent reactions may be written for the analogous deuterated compounds. There is some evidence that these are occurring in the nondeuterated system, but under most conditions they are of minor importance. This is not unexpected in view of the high activation energies for reactions 2*. Reaction 2b is expected to have a much larger activation energy than 2a and need not be considered. These reactions (2a, deuterated and nondeuterated) will be further considered in the discussion section. A measureable amount of 1-chloropropane was always present. A suggested mechanism is

$$CH_3 + H_2C{=}C{=}O \longrightarrow CH_3CH_2 + CO \qquad (3a)$$

$$CH_3CH_2 + CH_2Cl \longrightarrow CH_3CH_2CH_2Cl \qquad (3b)$$

and its deuterated counterpart.

Experimental combination ratios. The experimental combination ratios of $1,2\text{-}C_2H_4Cl_2/C_2H_5Cl$ and $1,2\text{-}C_2D_4Cl_2/C_2D_5Cl$ were obtained

*Alcock and Whittle (33) measured the activation of CF_3 radicals in reaction 2a as 10.6 kcal $mole^{-1}$ and estimated the activation energy for 2b to be 17 kcal $mole^{-1}$. Similar differences could be expected for methyl radicals.

from the high pressure limits of fig. 1. Steady state treatment of reactions 1 predicts

$$1,2\text{-}C_2H_4Cl_2/C_2H_5Cl = \frac{(k_1k_3)^{1/2}}{k_2}$$

for both nondeuterated and deuterated systems. The values taken from the graphs are 0.47 for the nondeuterated case and 0.52 for the deuterated case.

Collision theory gives this ratio as 0.5, which is the value normally found for cross combination (32). This is also evidence that H or D abstraction by CH_3 or CD_3 is minor (reaction 2a) at the high pressure conditions.

Assuming that $k_1 = k_3$ and using a steady state treatment for the radical concentration predicts that the ratio of ethane to 1,2-dichloroethane would be unity. As for the ratio of 1,2-dichloroethane to chloroethane, the ratio of ethane to chloroethane would be 0.5. The ethane to 1,2-dichloroethane ratio was suitable for direct analysis and the results are shown in Table I and Table II. For both cases at higher pressures the ratio is unity within experimental error. At lower pressures the nondeuterated system shows a real increase in this ratio; for the deuterated system it is fairly constant. This indicates the abstraction reaction (reaction 2a) may be playing an increasing role as the pressure is lowered in the nondeuterated system. This possibility will be further considered when the low pressure data are considered in the energy transfer section. It is unimportant for the determination of the unimolecular rate constants which is the next consideration.

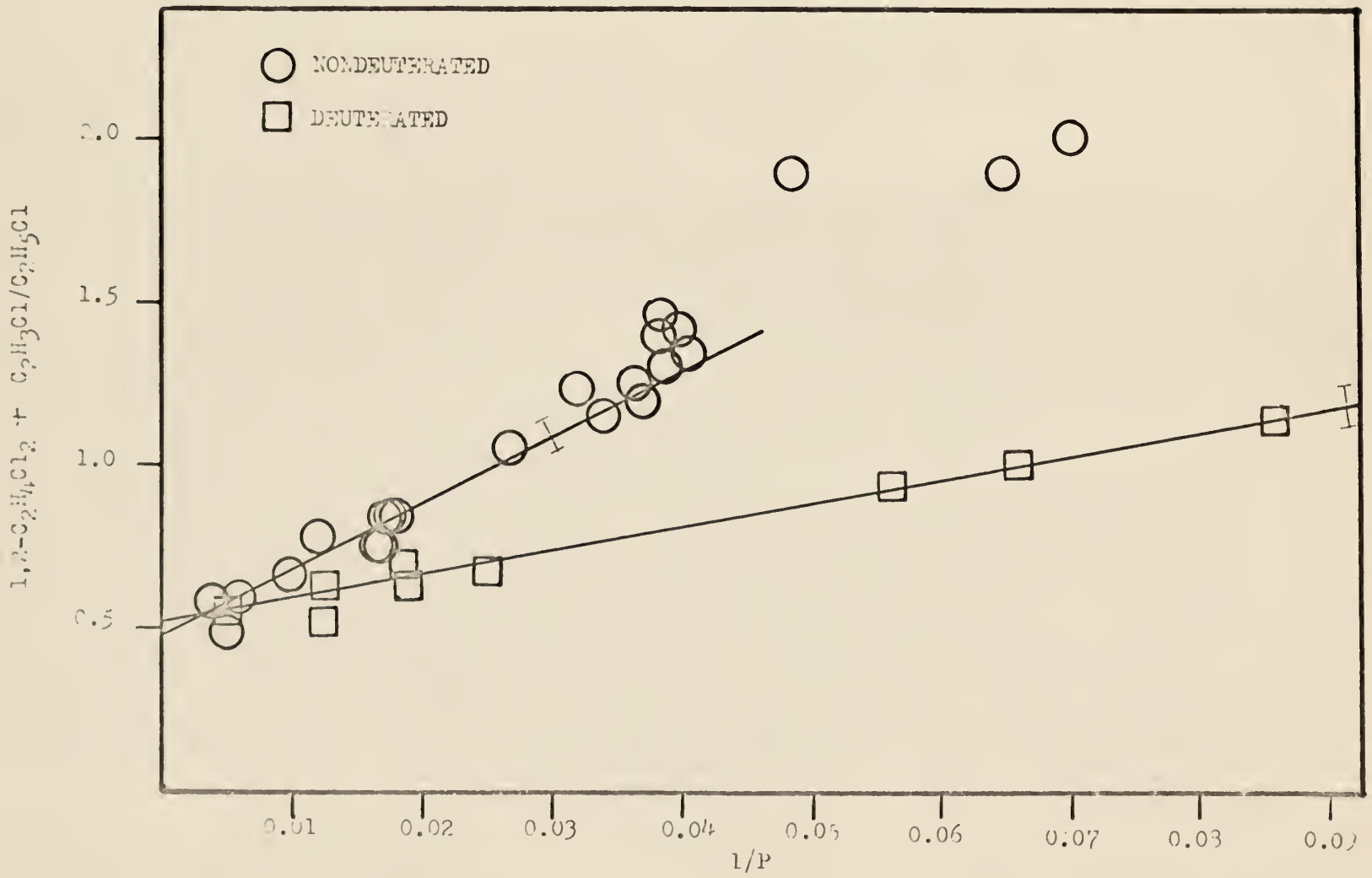

Fig. 1. $(1,2\text{-}C_2H_4Cl_2 + C_2H_4Cl/C_2H_5Cl)$ vs. 1/P (cm.)
The portion of the curve below the I mark was used for calculating the rate constant.

Isotopic purity. As indicated in the experimental section, a mass spectrographic analysis was made on the chloroethane, 1,2-dichloroethane, and ethane of the deuterated system. The isotopic purity was sufficient to neglect corrections to the rate constants for C_2D_5Cl and $C_2D_4Cl_2$.

Table I. Data of the ratio of nondeuterated ethane to nondeuterated 1,2-dichloroethane. All yields are gas phase volumes in cc at standard temperature and pressure.

Pressure (cm of Hg)	$C_2H_4Cl_2$ (cc)	C_2H_6 (cc)	C_2H_3Cl[a] (cc)	$\frac{C_2H_4Cl_2 + C_2H_3Cl}{C_2H_6}$
203.4	.0332	.0349	.0003	.96
55.6	.0273	.0250	.0008	1.12
37.0	.0283	.0238	.0013	1.24
31.2	.0239	.0199	.0013	1.27
26.9[b]	.0246	.0221	.0016	1.19
26.6	.0222	.0175	.0014	1.35
26.4	.0330	.0238	.0022	1.48
25.6	.0206	.0206	.0014	1.07
15.4	.0211	.0175	.0024	1.34
12.6	.0253	.0173	.0035	1.67
10.9	.0257	.0207	.0041	1.44
6.7	.0248	.0164	.0065	1.91
5.4	.0303	.0196	.0098	2.05
9.0	.0232	.0166	.0044	1.66
6.9	.0193	.0114	.0047	2.11

a. Vinyl chloride must be used in the ratio because it is a decomposition product of 1,2-dichloroethane. It was figured from the decomposition rate constant of 1,2-dichloroethane.

b. Pressures lower than this were not included in determining the decomposition rate constant.

Table II. Data of the ratio of deuterated ethane to deuterated 1,2-dichloroethane. All yields are in gas phase volumes in cc at standard temperature and pressure.

Pressure (cm of Hg)	$C_2D_4Cl_2$ (cc)	C_2D_6 (cc)	C_2D_3Cl[a] (cc)	$\frac{C_2D_4Cl_2 + C_2D_3Cl}{C_2D_6}$
79.2	.0268	.0236	.0002	1.14
17.8	.0273	.0263	.0008	1.07
9.9	.0271	.0277	.0014	1.03
8.1	.0156	.0176	.0010	.94
5.0[b]	.0225	.0204	.0023	1.22
3.6	.0205	.0188	.0029	1.25
3.6	.0166	.0178	.0023	1.06
2.5	.0161	.0145	.0032	1.33
2.4	.0168	.0178	.0023	1.17

a. Vinyl chloride must be used in the ratio because it is a decomposition product of 1,2-dichloroethane-d_4. Its contribution was figured from the decomposition rate constant of 1,2-dichloroethane-d_4.

b. Pressures lower than this were not included in determining the decomposition rate constants.

Nonequilibrium unimolecular rate constant for 1,2-dichloroethane-h_4 and 1,2-dichloroethane-d_4. The products of the exothermic combination reactions may undergo a unimolecular decomposition as the pressure is lowered. The intermediate pressure region will be defined, for this thesis, by pressures between 100 cm of Hg and pressures corresponding to points that fall on the linear parts of fig. 1 and fig. 2. Lower pressures than this will be discussed in the energy transfer section. The combination reactions 1d-1f are exothermic by an amount equal to the bond dissociation energy of the C-C bond or about 88 kcal $mole^{-1}$. Thus, the ethane, chloroethane, and 1,2-dichloroethane are vibrationally

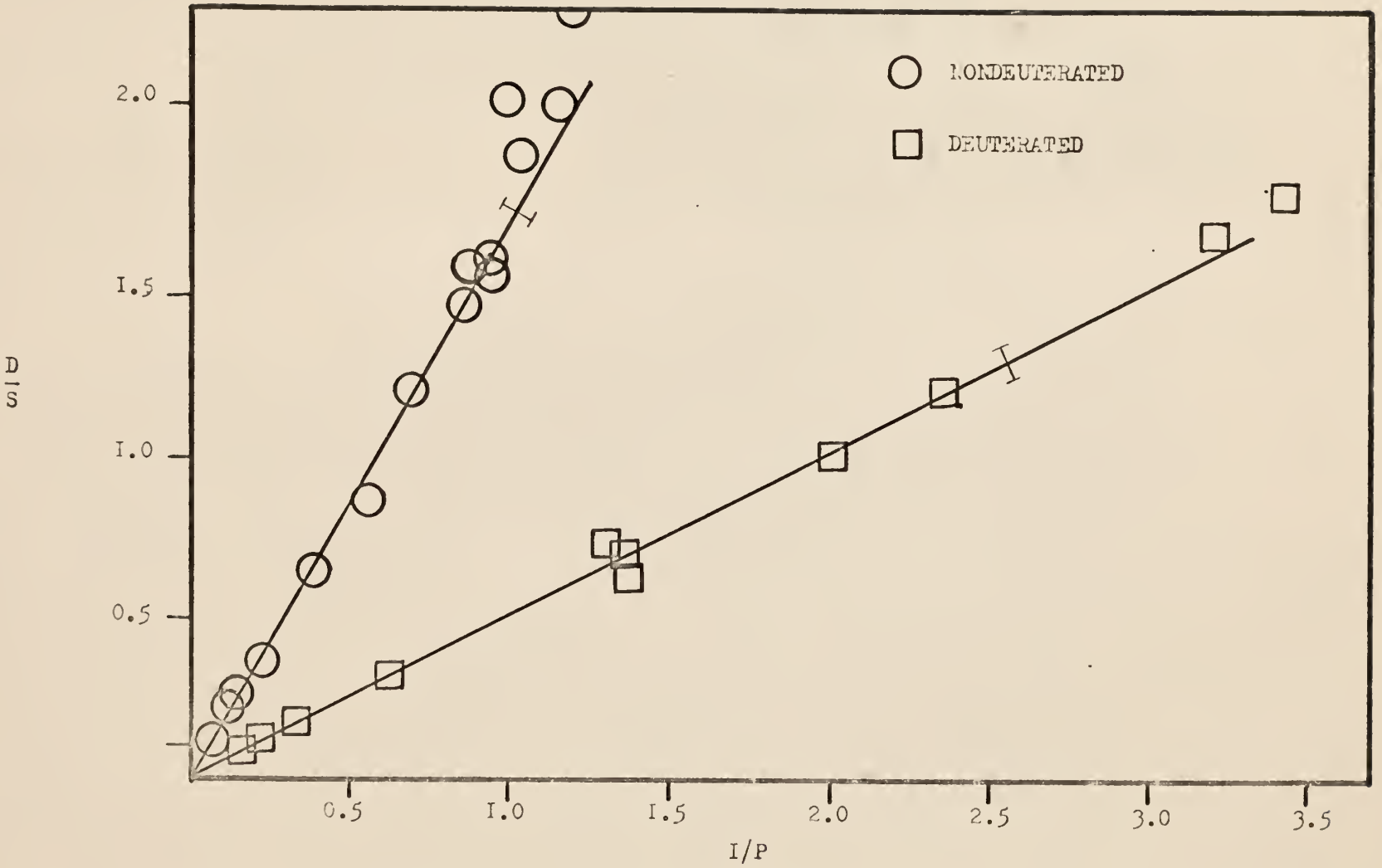

Fig. 2. $C_2H_3Cl/1,2\text{-}C_2H_4Cl_2$ (D/S) *vs.* 1/P (cm.)
The portion of the curve below the I mark was used for calculating the rate constant.

excited. Both chloroethane and 1,2-dichloroethane have an available reaction path of lower critical energy (= 55 kcal mole^{-1}) than either the reverse dissociation or Cl-atom rupture. This is the elimination of HCl with the formation of the corresponding olefin. The only reaction possible for ethane at these energies is dissociation and at 25 C, and pressures above 1 cm Hg this is not believed to be an important reaction (34). The reactions, for 1,2-dichloroethane believed to be occurring are

$$ClCH_2CH_2Cl^* \longrightarrow ClCH_2CH_2Cl \qquad (S_2) \qquad (4c)$$

$$\xrightarrow{k_{a2}} CH_2{=}CHCl + HCl \quad (D_2) \qquad (4d)$$

For the deuterated system the reactions would be the same except every hydrogen would be replaced by deuterium. The asterisk signifies vibrational excitation. S and D represent stabilized and decomposed products, respectively. The rate constants can be defined (35)

$$k_{ai} = (\omega\ D_i/S_i)$$

where i = 1 represents chloroethane and i = 2 represents 1,2-dichloroethane.

At lower pressures (defined in this thesis as low pressure region) less than perfect collisional efficiency produces a pressure dependent rate constant. One must therefore work above $S_i/D_i \geq .5$ to observe linear plots (36). A convenient measurement of the rate constants is in units of cm of Hg, i.e. the rate constant is equal to the pressure at which 1/2 the product is decomposed. This can be converted to sec^{-1} by the use of

collision diameters and the standard equation for collision frequency. The rate constant can be found by measurements of the ratio of decomposition to stabilization of products at different pressures in the intermediate pressure range. This is straightforward and a plot of D_2/S_2 vs. 1/P for $C_2H_4Cl_2$ and $C_2D_4Cl_2$ are shown in fig. 2. Table III shows representative data for these systems. Table VI shows a summary of these results and a ratio is given in the more common sec^{-1} units. The data are the results of a least squares analysis and the deviation are least squares deviations. The rate constants at 25 C are 1.73 $\pm$ .05 and 0.51 $\pm$ .01 cm of Hg for the deuterated and nondeuterated cases respectively.

An isotope effect can be determined by the ratio kH/kD, the rate constant of the nondeuterated species divided by the rate constant of the deuterated species, which is 3.48 $\pm$ .12 using sec^{-1} units.

Nonequilibrium unimolecular rate constant for chloroethane-h_5 and chloroethane-d_5. The product of chloroethane is ethene (reaction 4b).

$$C_2H_5Cl^* \xrightarrow{k_{a_1}} C_2H_5Cl \quad (S_1) \qquad (4a)$$

$$\xrightarrow{k_{a_1}} C_2H_4 + HCl \quad (D_1) \qquad (4b)$$

Ethene is also formed from the reaction of methylene with ketene (reaction 1b). This complication makes it impossible to directly obtain the rate constant from measured stabilized and decomposed products. An alternative expression is obtained by a steady state

Table III. Representative data for 1,2-dichloroethane-h_4 and 1,2-dichloroethane-d_4 decomposition. All yields are gas phase volumes in $cc(10^{-2})$ at standard conditions.

Pressure cm of Hg	C_2H_3Cl $cc(10^{-2})$	$C_2H_4Cl_2$ $cc(10^{-2})$	Pressure cm of Hg	C_2D_3Cl $cc(10^{-2})$	$C_2D_4Cl_2$ $cc(10^{-2})$
15.47	.22	1.98	72.3	.07	.257
8.57	.35	1.50	58.1	.007	.284
7.98	.58	2.63	20.42	.008	.204
6.87	.35	1.37	17.88	.012	.256
4.44	.45	1.23	15.99	.011	.210
2.56	.90	1.40	7.81	.014	.190
1.80	1.28	1.47	5.78	.018	.193
1.46	1.22	1.01	4.62	.013	.106
1.17	2.27	1.54	3.00	.014	.077
1.15	1.95	1.21	1.60	.622	2.035
1.06	2.40	1.47	.940	.065	.120
1.03	1.61	1.03	.757	.109	.079
.99	2.75	1.32	.736	1.07	1.52
.99	2.09	1.18	.499	1.45	1.42
.97	1.80	.975	.722	.073	.120
.86	1.79	.890	.422	1.67	1.36
.83	2.03	.855	.312	1.26	.731
.70	2.50	.872	.291	.110	.064
.67	2.80	.742	.247	1.75	.711
.56	3.02	.836	.209	2.01	.721
.50	1.89	.378	.166	1.70	.435
.35	1.28	.171	.144	1.86	.445
.32	.744	.903	.097	1.71	.276
.30	3.68	.275	.078	1.55	.208
.20	3.36	.192	.069	1.57	.162
.17	3.28	.155			
.16	4.16	.155			
.12	3.13	.084			

treatment of equations 4. This gives

$$(1,2\text{-}C_2H_4Cl_2 + C_2H_3Cl)/(C_2H_5Cl) = I(1 + ka_1/P)$$

where I is the intercept given by $\frac{(k_1k_3)^{1/2}}{k_2}$. If $(1,2\text{-}C_2H_4Cl_2 + C_2H_3Cl)/C_2H_5Cl$ is plotted vs. 1/P, the intercept is I and k_{a1} = constant (slope/I). The constant is the conversion factor from units of cm of Hg to sec^{-1}. Such a plot of both nondeuterated and deuterated cases is shown in fig. 1. Table IV and V contain representative data from these systems. The linear portions of the curves (indicated in fig. 1) were used to obtain the rate expression. The deviation from linearity will be discussed in the energy transfer section.

The rate constants by least square treatment are 42.3 $\pm$ 4.2 and 12.7 $\pm$ 0.56 cm for chloroethane-h_4 and chloroethane-d_4, respectively. This method of obtaining the rate constant assumes that the ratio of formed $[C_2H_4Cl^*]/[C_2H_5Cl^*]$ is independent of pressure. The method to be discussed below also utilizes this assumption in a slightly different way.

These rate constants were checked by another method of evaluating the rate constant. Since steady state treatment predicts

$$1,2\text{-}C_2H_4Cl_2/C_2H_5Cl = (k_1k_3)^{1/2}/k_2$$

and since this high pressure intercept is known (see experimental combination ratios) it is possible to calculate the expected quantity of decomposition product from analysis of $1,2\text{-}C_2H_4Cl_2$

Table IV. Representative data for chloroethane-h_5 decomposition. All yields are gas phase volumes in cc (10^{-2}) at standard conditions.

Pressure cm of Hg	C_2H_5Cl cc(10^{-2})	1,2-$C_2H_4Cl_2$ cc (10^{-2})	C_2H_3Cl[a] cc(10^{-2})
283.	3.80	2.24	.014
203.	6.62	3.32	.028
186.	3.26	1.82	.017
101.	2.14	1.39	.024
82.3	2.92	2.20	.046
63.4	2.20	1.61	.044
57.7	1.70	1.39	.024
56.2	2.46	1.96	.060
55.6	3.35	2.73	.085
37.1	1.49	1.47	.068
37.0	2.85	2.83	.132
31.2	2.02	2.39	.132
29.5	1.76	1.91	.112
26.6	1.93	2.22	.145
26.4	2.24	2.93	.192
26.4	2.41	3.30	.216
25.6	1.70	2.06	.139
25.2	2.09	2.76	.190
24.5	1.63	2.05	.144
20.4	1.37	2.43	.206
19.1	1.70	2.08	.189
15.4	1.23	2.11	.237
14.6	1.12	2.59	.307
14.2	1.15	2.14	.261
12.6	1.10	2.53	.347
10.9	1.02	2.57	.409
9.03	.714	2.31	.443
6.92	.377	1.93	.483
6.65	.207	2.48	.643
5.37	.450	3.03	.977

a. These values were calculated from the decomposition rate constant of 1,2-$C_2H_4Cl_2$.

Table V. Representative data for chloroethane-d_5 decomposition. All yields are gas phase volumes in cc (10^{-2}) at standard conditions.

Pressure cm of Hg	C_2D_5Cl cc(10^{-2})	1,2-$C_2D_4Cl_2$ cc(10^{-2})	C_2D_3Cl[a] cc(10^{-2})
194.	4.47	2.39	.006
79.7	3.73	2.36	.015
79.2	5.58	2.80	.018
53.0	4.02	2.74	.026
38.8	2.68	1.76	.023
17.8	3.01	2.73	.078
15.1	1.65	1.78	.078
11.6	1.63	1.78	.078
9.98	2.29	2.54	.130
9.11	1.70	1.99	.111
7.22	.814	1.10	.078
5.50	1.88	2.95	.274
4.55	.644	1.47	.164
3.64	.687	1.66	.233
3.58	.66	2.05	.292
2.54	.37	1.61	.323
2.37	.38	1.68	.362

a. These values were calculated from the decomposition rate constant of 1.2-$C_2D_4Cl_2$.

and C_2H_5Cl by the following equation:

$$\frac{1,2\text{-}C_2H_4Cl_2 + C_2H_3Cl}{C_2H_5Cl + C_2H_4} = .47$$

The analogous equation exists for the deuterated system. The vinyl chloride is obtained from the 1,2-dichloroethane decomposition rate constant and the measured $C_2H_4Cl_2$. The only unknown left is ethene and this is calculated from the intercept equation. Ethene/chloroethane vs. 1/P is then plotted directly and the slope is the rate constant. Such a plot for both the deuterated and nondeuterated case is shown in fig. 3. The rate constants are 40 cm and 12.7 cm for the chloroethane-h_5 and chloroethane-d_5, respectively. This is in good agreement with the first method. Since the chloroethane-h_5 rate constant is slightly different for the two methods the average of 41 cm was taken as the best value. Table VI shows the results in summary.

The isotope effect k_H/k_D is $3.33 \pm .38$ using units of sec^{-1}.

Collision deactivation models-low pressure region energy transfer. For unit deactivation efficiency, the systems (deuterated and nondeuterated) are adequately described by equations 4a-4d

$$C_2H_5Cl^* \xrightarrow{\omega} C_2H_5Cl \qquad (S_1) \qquad (4a)$$

$$\xrightarrow{k_{a1}} C_2H_4 + HCl \qquad (D_1) \qquad (4b)$$

$$ClCH_2CH_2Cl^* \xrightarrow{\omega} ClCH_2CH_2Cl \qquad (S_2) \qquad (4c)$$

$$\xrightarrow{k_{a2}} CH_2 = CHCl + HCl \qquad (D_2) \qquad (4d)$$

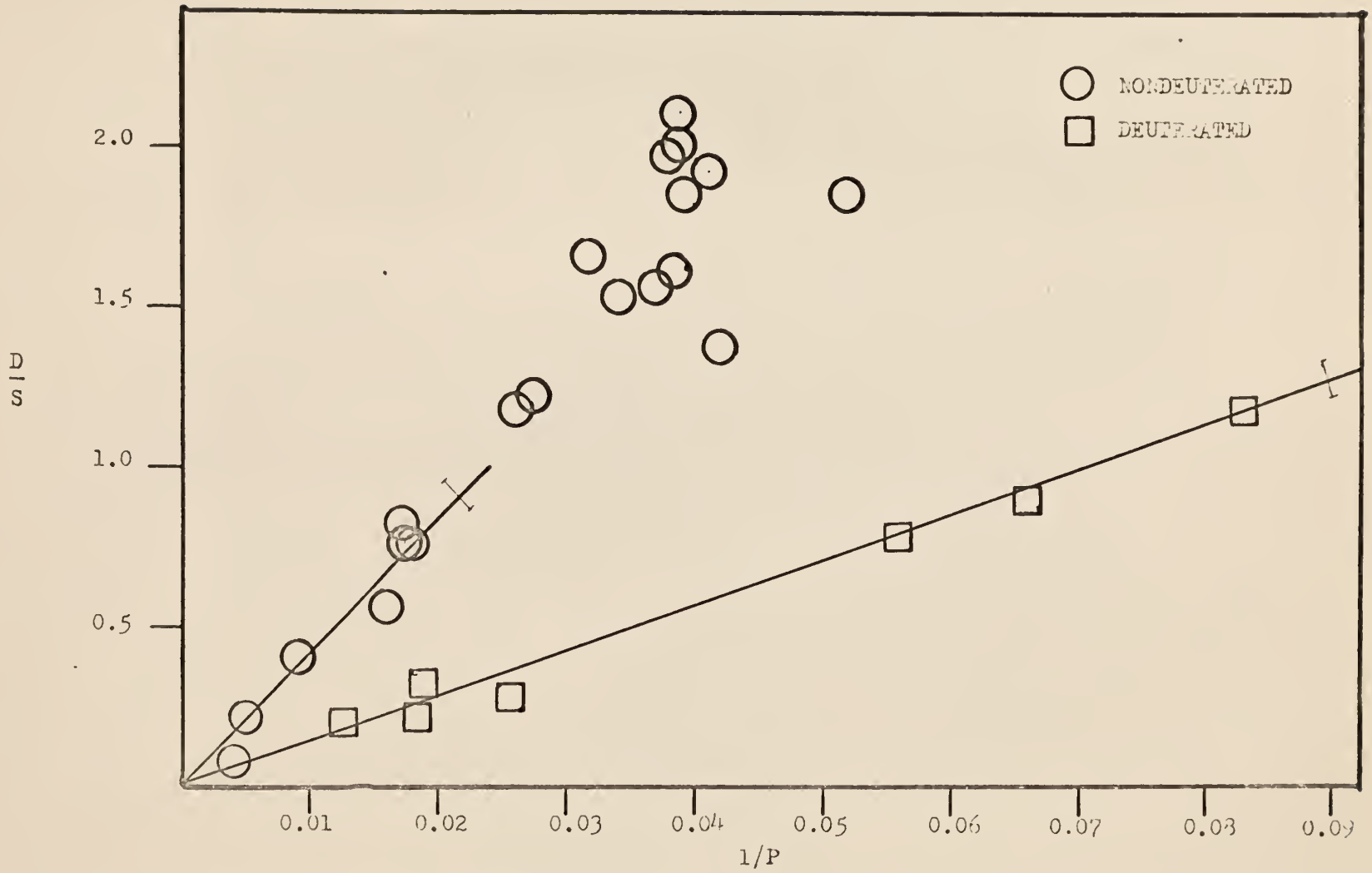

Fig. 3. C_2H_4/C_2H_5Cl (D/S) *vs.* 1/P (cm.)
The portion of the curve below the I mark was used for calculating the rate constant.

Table VI. Experimental rate constants for the nonequilibrium unimolecular elimination of HCl or DCl from chemically activated molecules.

Molecule	Units of cm of Hg	Units of sec^{-1} [a]	Ratio (sec^{-1})
C_2H_5Cl	41.0 ± 4.2	4.63×10^9	3.33 ± .38
C_2D_5Cl	12.7 ± .56	1.39×10^9	
1,2-$C_2H_4Cl_2$	1.73 ± .05	1.99×10^8	3.48 ± .12
1,2-$C_2D_4Cl_2$	0.51 ± .01	5.71×10^7	

[a] Collision cross sections (11,37) for CH_3Cl, C_2H_5Cl, and $C_2H_4Cl_2$ are 4.2, 5.5, and 6.0 A respectively. The same cross sections were used for the deuterated species.

and the analogous deuterated equations. If collisional inefficiency is introduced (less than unit deactivation) equations 4b and 4d are no longer adequate and an energy transfer model must be formulated. In the low pressure region this collisional inefficiency was observed, but this does not affect the previously discussed experimental data in the high and intermediate pressure regions because the rate constants are insensitive to the exact collision mechanism for $S/D \geq 0.5$. (36,38) For inefficient deactivation the definition of the rate constant, $k = \omega D/S$, is still valid, it just becomes pressure dependent in the low pressure region. The collisional deactivation model is next outlined.

The steady-state transport equations which describe (7) the system are

$$dn_i/dt = \omega(\Sigma_j P_{ij} n_j - \Sigma_j P_{ji} n_i) - k_{ei} n_i + Rf_i = 0 \qquad (5)$$

or

$$dn_i/dt = \omega(\Sigma_{j \neq i} P_{ij} n_j - (k_{ei} + \beta_i \omega) n_i + Rf_i = 0 \qquad (6)$$

where P_{ji} is the probability per collision that a molecule in state i will undergo a transition to state j, so that $\Sigma_j P_{ji} = 1$;

n_i is the steady-state population of the ith state;

β_i is the effective collision factor $(1-P_{ii})$; then $\beta_i = 1$, if $P_{ii} = 0$; β_i is taken constant for all i, equal to β;

$k_{\varepsilon i}$ is the specific decomposition probability per second for state i;

R is the total rate of chemical activation; and

f_i is the activation distribution function, with the normalization $\Sigma_i f_i = 1$.

The expressions for decomposition D and stabilization S are

$$D = \Sigma k_i n_i \qquad S = R - \Sigma k_i n_i \tag{7}$$

The simple stepladder cascade model will be used. For such a model energy losses per collision, $\Delta\varepsilon = S$ kcal mole^{-1}, are of constant size and up transitions are not allowed. The collision probabilities become

$$P_{ij} = 1 \qquad j - 1 = S$$

$$P_{ij} = 0 \qquad j - 1 \neq S$$

and $P_{ii} = 0$ is assumed. If T is the number of transitions in the active region, then the equations reduce to

$$S_T = \prod_{t=1}^{T} \left(\frac{\beta\omega}{\beta_\omega + k_\varepsilon} \right) \qquad D_T = 1 - S_T \tag{8}$$

and

$$k_a = \omega \frac{D_T}{S_T} = \omega (1/\beta\omega)^T \prod_{t=1}^{T} (\beta_\omega + k_\varepsilon) - 1 \tag{9}$$

From knowledge of the initial distribution function and the values of k_ε calculated using RRKM formulation it is possible to compute values of S/D and k_a at various pressures. The pressure dependence of the rate constants can be used to estimate the value of S when the results are compared to the experiments. The theoretical curves are shown in fig. 4 and fig. 5 and are compared to the experimental points in those plots.

1,2-dichloroethane. Fig. 4 shows the experimental k/k_∞ plotted vs. S/D. The solid line shows the theoretical curves from the above model for $C_2H_4Cl_2$. For a given energy jump size the theoretical curve for the deuterated system corresponds to a 1-1.5 kcal $mole^{-1}$ larger jump size for the nondeuterated case. This effect is shown by the broken line in fig. 4 for a 10.9 kcal $mole^{-1}$ jump size and arises because the k_ε for C_2H_5Cl varies differently as a function of energy than the k_ε for C_2D_5Cl. Experimental difficulty made it impossible to extend the experimental deuterated graphs to any lower pressure; the main problem is that the yields fall with decreasing pressure. The important thing to note is that within experimental error the graphs for the experimental data for the deuterated and nondeuterated cases are nearly identical, i.e. they fall on top of one another. Since the experimental data are scattered, the best jump size to fit both the deuterated and nondeuterated experimental data was judged the same; 12-14 kcal $mole^{-1}$ per collision gives a fairly good fit.

Chloroethane. At lower pressures the deviations from linearity of fig. 2 may be due to two effects; the $C_2H_5Cl^*$ yield

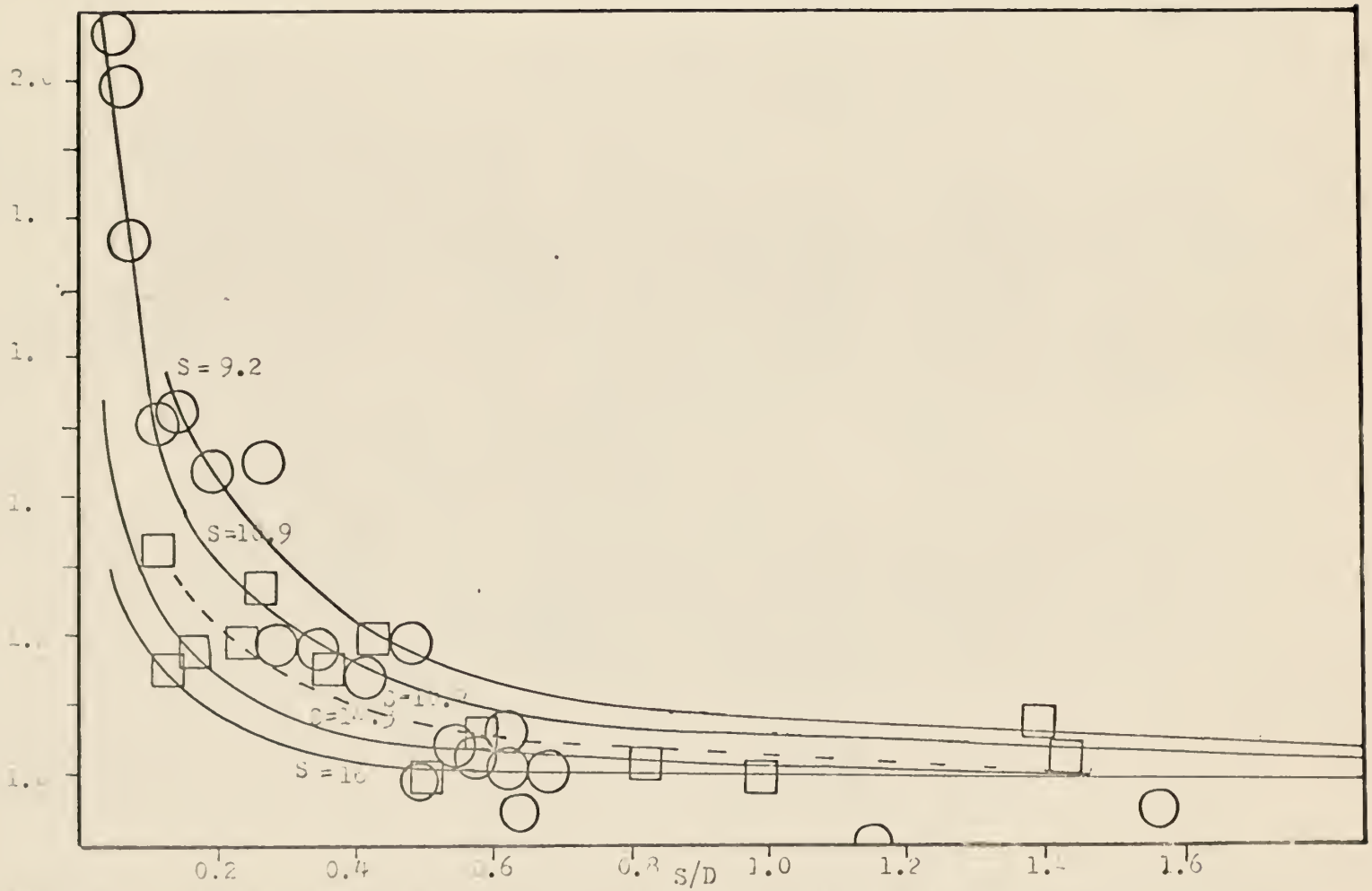

k/k_∞ vs. S/D for deuterated and nondeuterated 1,2-dichloroethane. The solid lines are theoretical curves calculated from a simple cascade model for $C_2H_4Cl_2$. The broken line is the theoretical curve for $C_2D_4Cl_2$. Jump sizes are indicated by S.
□ = deuterated; ○ = nondeuterated.

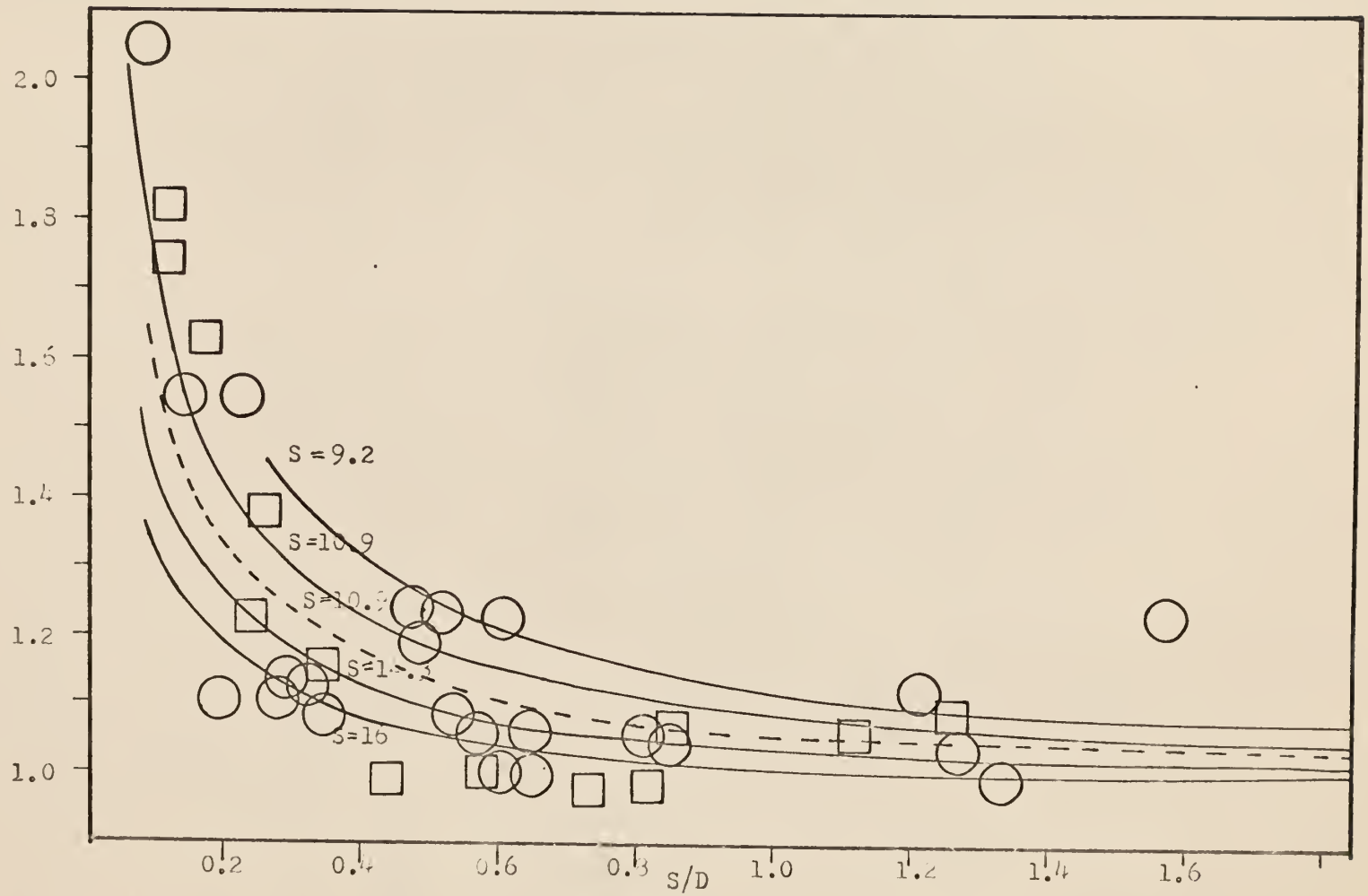

Fig. 5. k/k_δ vs. S/D for deuterated and nondeuterated chloroethane. The solid lines are theoretical curves calculated from a simple cascade model for C_2H_5Cl. The broken line is a theoretical curve for C_2D_5Cl. Jump sizes are indicated by S.
□ = deuterated; ○ = nondeuterated

may be lowered because the CH_3 radical concentration may be decreased relative to the CH_2Cl concentration by the abstraction reaction (2a), and the collisional efficiency may be less than perfect as discussed in the general section above. The ratio ethane/1,2-dichloroethane which is given by $k_1(CH_3)^2/k_3(CH_2Cl)^2$ indicated that for the deuterated reactions the abstraction reactions are not important over the pressure range from 79 to 3.6 cm. For the nondeuterated reactions this is not the case. The ratio became somewhat greater as the pressure was lowered. However, the deviation is not great. Since the ratio depends upon the radical concentration squared, this is a sensitive test and a deviation of approximately 10% occurs in the ratio of CH_3/CH_2Cl. The strong dependence of the rate constants upon pressure are, therefore, attributed to energy transfer effects. Our methods of analysis produced scatter in the nondeuterated system. Reasons for this are not fully understood, however, and the abstraction reaction (2a) may be partly responsible. It should be noted that this difficulty with the abstraction reaction arose because of the inability to measure D/S directly for chloroethane.

Since the deviation in concentration for the nondeuterated case due to abstraction reactions is not great, the nondeuterated and deuterated reactions can be compared in the low pressure region. Within experimental error, the nondeuterated and deuterated experimental results are identical. The data will again by analysed using a simple stepladder model for the rate constants. As with the 1,2-dichloroethane system, the chloroethane computed stepladder curves display a 1-1.5 kcal $mole^{-1}$ shift or the energy

jump size to match the energy jump size curves for the non-deuterated system. This effect is shown by the broken line in Fig. 5 for a jumpsize of 10.9 kcal $mole^{-1}$. Again a computed jump size of 12-14 kcal $mole^{-1}$ fits the experimental data for deuterated and nondeuterated systems fairly well.

DISCUSSION

General

It should be emphasized that the objective of this work was to measure nonequilibrium unimolecular kinetic isotope effects. The nondeuterated case was thoroughily studied previously (8,9). This work utilized a new analytical technique which appears to be better than that of the earlier study. The earlier research was repeated in order to get a fair comparison of the rate constants for the deuterated and nondeuterated molecules under the same conditions. This research, however, was compared to the earlier results whenever possible and was found to substantiate them. The deuterated reactions behaved very much the same as the nondeuterated reactions except for the expected kinetic isotope effects upon the rate constants. The discussion section will be divided into two parts. First the experimental results are considered and next these results are used to test various models of the HCl elimination reactions. Details which are important in the calculations but not necessary to the understanding of the general conclusions are presented in appendices.

Experimental Results

Experimental rate constants. Earlier research (8,9) from this lab placed the C_2H_5Cl decomposition rate constant as 27 cm compared to 41 cm found here. The deviation is largely unexplained. The two values probably represent the upper and lower limits to the rate constant. Actually the estimated error for

the earlier measurements encompasses the present findings. Johnstone and Wayne (39) have reported two values for the decomposition of C_2H_5Cl. They believe that the radicals forming the molecule were not "thermalized" before combining, thus the molecule was formed with different amounts of average energy depending upon the amount each radical carried into the combination reaction. They report k_{a1} as 24.2 cm Hg (2.73×10^9 sec^{-1}) and 39 cm Hg (4.41×10^9 sec^{-1}) as a result of photolysis of ketene in the spectral regions $\lambda \approx$ 2600A - 3200 A and $\lambda \approx$ 3220-3800 A, respectively. Our observations have shown that below a pressure of $\approx$ 30 cm, k_{a1} becomes a function of pressure because the strong collision assumption is not obeyed. Another possible factor is that the C_2H_6/C_2H_5Cl ratio measured by these authors may become pressure dependent due to radical abstraction as found in the work. The measured C_2H_6/C_2H_5Cl ratio for these authors work includes pressures down to $\approx$ 10 cm. They apparently found no pressure dependence of the rate constant with decreasing pressure but the data are not extensive. They used a 1:1.6 ratio of ketene to chloromethane where our work utilized a 1:10 ratio. However, both chloromethane and ketene should be efficient stabilizers and this difference would not explain why their ratio changed from one wavelength to another. Fortunately, we have measured the rate constant for $C_2H_4Cl_2$* under a variety of conditions and accurate measurement of D and S permits reliable evaluation of the rate constant. The same value is always obtained with different activation techniques thus ruling out non-thermalized CH_2Cl radicals under our experimental conditions, and CH_3 should behave the same way.

The $C_2H_4Cl_2$ rate constant for the earlier research (8,9) was 1.8 compared to 1.73 cm for this research, thus being in good agreement. The rate constants given in table VI are the result of a least squares determination. The least squares deviations given are somewhat misleading, because systematic errors in gas-chromatography are rather large. It is estimated that more reliable limits are $\pm$ 30% for all the rate constants.

The rate constants for the C_2H_5Cl and C_2D_5Cl molecules were indirectly measured for the reasons mentioned earlier, i.e. the decomposition product ethene is also produced by another reaction (reaction 1b). In plotting 1,2-dichloroethane + vinyl chloride/chloroethane vs. 1/P, to obtain the rate constant (slope/intercept) the assumption is that the ratio of concentrations of CH_3 and CH_2Cl are independent of pressure between the highest pressure used and about 27 cm for the nondeuterated case and about 5 cm for the deuterated case. This infers that the abstraction reactions 2a-2b do not occur in this pressure range. The ratio of 1,2-dichloroethane to ethane (see combination ratio section) is a sensitive monitor of this assumption because the radical concentrations are squared in the product ratio. As indicated in the combination ratio section this ratio seems to hold for the deuterated case but deviates for the nondeuterated case as the pressure is lowered. Sharp and Johnson (40) report that k_H abstraction is approximately 16 times greater than k_D abstraction on a per atom basis at 25 C in CF_3 + CHD_3 system. If a similar rate constant is assumed in our systems, H abstraction but not D abstraction is understandable.

Experimental isotope effects. Large normal intermolecular secondary isotope effects in unimolecular systems having a non-equilibrium distribution of energized species have been found for a variety of compounds by Rabinovitch and coworkers. The magnitude of the isotope effects were shown to depend on the degree of isotopic substitution, on the average energy of the energized species and on ε_o, the critical energy for reaction. Some of these results will now be examined to show how the chloroethane data qualitatively fit the previous trends. The secondary effect studies with ethyl radicals (20,21) have involved critical energies in the region = 40 kcal mole^{-1} with a few kcal mole^{-1} excess energy ($\langle\varepsilon^+\rangle$). For the ethyl-$d_1$:ethyl-$d_3$ chemically activated radical system the total intermolecular* secondary effect for H rupture at 300 K was k_H/k_D = 3. The isotope effect for decomposition of chemically activated butyl-d_1:butyl-d_9 and butyl-d_0:butyl-d_8 (19,24) by C-C rupture with ε_o = 33 kcal mole^{-1} and $\langle\varepsilon^+\rangle$ = 10 kcal mole^{-1} gave a total normal secondary isotope effect of $(\frac{kH}{kD})$ = 3.6-4.3 at 300 K. Chemically activated n-propyl-d_0:n-propyl-d_6 decomposition (25) by a C-C rupture at an average energy of 37.3 kcal mole^{-1} and ε_o = 31 kcal mole^{-1} at 298 K resulted in $(\frac{kH}{kD})$ = 4.5. The primary as well as secondary intermolecular isotope effect was analyzed (23) for the photosensitization of C_2H_4 and C_2D_4 and the resulting H_2 or D_2 split off. At 298 K a total rate constant ratio was partitioned as follows: $(\frac{kH}{kD})$ = 4.1, $(\frac{kH}{kD})$ primary = 2, $(\frac{kH}{kD})$ secondary = 2, $\langle\varepsilon^+\rangle$ was guessed at 19 kcal mole^{-1} and ε_o in the neighborhood of 93-112 kcal mole^{-1}. A study of the geometric and structural

*See ref. 22 for an intramolecular effect.

isomerization reactions of chemically activated cis-1,2-dimethylcyclopropane-d_0 & d_8 (26) resulted in information on pure secondary and mixed primary and secondary isotope effects. For example $\frac{kH}{kD}$ for structural isomerization (secondary effect) = 4.3, ε_o = 60 kcal mole^{-1} and $\langle\varepsilon^+\rangle$ = 40 kcal mole^{-1}.

As the examples above indicate, most work has been done for ε_o in the 30-40 kcal mole^{-1} and the corresponding $\langle\varepsilon^+\rangle$ = 1-10 kcal mole^{-1} and ε_o in the 60 kcal mole^{-1} range and the corresponding $\langle\varepsilon^+\rangle$ = 46 kcal mole^{-1}. The present work has an ε_o = 55 kcal mole^{-1} and $\langle\varepsilon^+\rangle$ = 36 kcal mole^{-1}, being somewhere intermediate in values from previous studies. This is the first nonequilibrium study with a halogen atom in the molecule and the first study for a four centered reaction. Since the chloroethane molecules have relatively few isotopically substituted atoms (d_5 compared to say d_8) and $\langle\varepsilon^+\rangle$ is large, which does not favor a secondary effect, the large measured kinetic isotope effects of = 3.4 must include contributions from a primary as well as secondary effect. Calculations and speculations on this are presented later.

The only pertinent thermal <u>intermolecular</u> isotope study is chloroethane-d_0 and chloroethane-d_5 pyrolysis by Heydtmann and Volker (18). These results are used extensively in the calculations section. Intramolecular studies have been reported on cyclopropanes (41) and cyclobutanes (42) and haloethanes (17, 43, 44). Such studies are very useful for fixing properties of the activated complexes because the properties of the molecule cancel from the k_H/k_D ratio. Of particular importance to this study is the intramolecular kinetic isotope effect in the pyrolysis of ethyl 1,1,2,2-d_4 chloride (17).

Qualitative considerations of the energy transfer data. Recent data* indicate that relatively large quantities of energy are removed from a highly vibrationally excited polyatomic molecule upon each collision. For example ethylene (45) removes in excess of 10 kcal $mole^{-1}$ per collision with chemically activated cyclopropane (100 kcal $mole^{-1}$ above ground level). Helium will remove up to 6 kcal $mole^{-1}$ from cyclopropane. H_2 and D_2 will remove ≈ 1.3 kcal $mole^{-1}$ from chemically activated sec-butyl radicals (46). Chemically activated 1,2-dichloroethane-d_0 has been previously (28) studied with deactivators such as CH_3Cl and Ar. It was found 10 kcal $mole^{-1}$ and ≈ 6 kcal $mole^{-1}$ was removed per collision, respectively. This study has now been extended to deuterated 1,2-dichloroethane using CD_3Cl as the deactivator and chloroethane-d_0 & d_5 using CH_3Cl and CD_3Cl as deactivators, respectively. The main purpose was to find if the deuterated molecules followed the same deactivation scheme as the nondeuterated ones. Since the deuterated species have a much larger density of states (≈ a factor of 30 in the energy range of ≈ 90 kcal $mole^{-1}$ to 75 kcal $mole^{-1}$), even though all other characteristics of the molecules such as collision diameter, etc. are the same, it is possible that the deactivation mechanism could differ. Different deactivators were used for the nondeuterated as compared to the deuterated case so the energy level density is not an isolated parameter but it should be the main difference. The results, using a stepladder deactivation model, since the experimental data is not sufficiently good to warrant comparison of

*Adequately reviewed in ref. 7.

different models, indicate that for these molecules the different densities did not effect the jump size. The experimental S/D vs. k/k_∞ are within experimental error, the same for C_2H_5Cl and C_2D_5Cl system and the $C_2H_4Cl_2$ and C_2D_4Cl system.

Computational Procedure

Goals. The main purpose of this section is to develop models for HCl and DCl elimination reactions using the RRKM formulation (4, 5,6) of unimolecular reactions from which rate data may be computed and compared to the experimental results. The model may be fitted to both nonequilibrium and thermal equilibrium kinetic data. The thermal kinetic systems have a Boltzman distribution of energies for the activated molecule which may be characterized by the temperature; the nonequilibrium systems have some nonequilibrium distribution of energies characterized by the method of activation. The model for the reaction will be judged relative to obtaining correct $\frac{k_aH}{k_aD}$ (nonequilibrium) and $\frac{k_{cond}}{k_{\infty D}}$(thermal) ratios and also the absolute fit to the rate constants for chloroethane. The lack of sufficient thermochemical and molecular structure information for the dichloroethane prevents quantitative comparison of calculated to experimental measurement for the dichloroethanes.

Specific rate constant and general expressions. The application of the RRKM formulation of unimolecular reactions to nondeuterated chloroethanes has been previously presented in detail (2); the equations are merely summarized here The specific rate constants as a function of energy are given by

$$k_\varepsilon = \frac{\sigma}{h} \frac{Z_1^+}{Z_1^*} \frac{\Sigma p(\varepsilon_{vr}^+)}{N^*(\varepsilon_{vr})} \qquad (10)$$

σ is the reaction path degeneracy;

Z_1^+ is the products of partition functions for the adiabatic degrees of freedom for the complex;

Z_1^* is the products of partition functions for the adiabatic degrees of freedom for the molecule;

$\Sigma p(\varepsilon_{vr}^+)$ is the total sum of the degeneracies of all possible energy eigenstates of the active degrees of freedom of the complex at energy ε_{vr}^+ ;

$N^*(\varepsilon_{vr})$ is the number of eigenstates per unit energy (density of states); for the active degrees of freedom of the molecule at energy ε_{vr};

h is Planks constant;

ε_o is the minimum energy necessary for reaction (critical energy); and

$\varepsilon_{vr}^+ = \varepsilon_{vr} - \varepsilon_o$ where ε_{vr} is the total energy.

The numerical values of k_ε are obtained from computer computations using molecular models of the complex and molecule. These details are described in appendix I but the main features are summarized below. For a monoenergetic system following unit deactivation

$$\text{formation} \longrightarrow M^* \xrightarrow{k_\varepsilon} \text{products} \qquad (D)$$

$$M^* \xrightarrow{\omega} M \qquad (S)$$

and for such model $k_\varepsilon = \omega D/S = k_a$. For a particular nonequilibrium activation technique which gives an energy distribution function,

$f(\varepsilon)$, the rate constant has the form

$$k_a = \omega\, D/S = \omega \frac{\int_{\varepsilon_o}^{\infty} \frac{k_\varepsilon}{k\varepsilon+\omega} f(\varepsilon)\, d\varepsilon}{\int_{\varepsilon_o}^{\infty} \frac{\omega}{k_\varepsilon+\omega} f(\varepsilon)\, d\varepsilon} \tag{11}$$

The absolute magnitude of k_a depends upon the model of the complex and molecule and the level of energy of the molecule. The nonequilibrium isotope effect then becomes

$$\frac{ka_H}{ka_D} = \frac{\int_{\varepsilon_{oH}}^{\infty} \frac{k_{\varepsilon H} f(\varepsilon)_H\, d\varepsilon}{K_{\varepsilon H}+\omega}}{\int_{\varepsilon_{cH}}^{\infty} \frac{\omega f(\varepsilon)_H\, d\varepsilon}{k_{\varepsilon H}+\omega}} \cdot \frac{\int_{\varepsilon_{oD}}^{\infty} \frac{\omega f(\varepsilon)_D\, d\varepsilon}{k_\varepsilon D+\omega}}{\int_{\varepsilon_{oD}}^{\infty} \frac{k_{\varepsilon D} f(\varepsilon)_D\, d\varepsilon}{k_{\varepsilon D}+\omega}}$$

where subscripts H and D are used to designate the isotopic species. Before worrying about the distribution function it is instructive to consider a simplified form. The simplest form of $f(\varepsilon)$ is a delta function and it permits the characteristics of the above ratio to be readily exhibited.

$$\frac{k_{\varepsilon H}}{k_{\varepsilon D}} = \frac{I_{rH}}{I_{rD}} \left[\frac{\sum_{\varepsilon_{vr}^{+}=0}^{\varepsilon-\varepsilon_o} p(\varepsilon_v^{+})H}{\sum_{\varepsilon_{vr}^{+}=0}^{\varepsilon-\varepsilon_o} p(\varepsilon_v^{+})D} \right] \left[\frac{N_{\varepsilon D}^{*}}{N_{\varepsilon H}^{*}} \right] \tag{12}$$

I_r is a residue of moments of inertia of rotational partition functions of the molecule and activated complex. Let us assume a complete vibrational model, i.e. there are no internal rotation, which is the appropriate description of the models discussed in

this thesis. Both the activated complex sum and the molecule density for the deuterated species are larger than those for the light species because the more closely spaced energy levels of the former. Hence the sum ratio of Equation 12 is less than unity while the densities ratio is greater than unity; the I_r ratio is approximately unity. The maximum isotope effects that can be expected are next considered.

A maximum secondary effect for a particular system occurs as $\langle \varepsilon^+ \rangle \to 0$ or

$$\Sigma P(\varepsilon_v^+)_H \simeq \Sigma P(\varepsilon_v^+)_D \simeq 1$$

For example the density of states ratio for C_2H_5Cl and C_2D_5Cl are given in the following table in 1500 cm^{-1} increments and if $\varepsilon_o H = \varepsilon_o D$ and $\varepsilon^+ = 0$ these ratios would be the isotope effects.

Table VII. Density of states for C_2H_5Cl and C_2D_5Cl molecules[a]

energy cm^{-1}	kcal	C_2H_5Cl density $(cm^{-1})^{-1}$	C_2D_5Cl density $(cm^{-1})^{-1}$	ratio
20000	57.18	2.24×10^6	5.29×10^7	23.6
21500	61.46	4.91×10^6	1.24×10^8	25.3
23000	65.75	1.04×10^7	2.80×10^8	26.9
24500	70.04	2.13×10^7	6.06×10^8	28.5
26000	74.33	4.22×10^7	1.27×10^9	30.1
27500	78.62	8.15×10^7	2.57×10^9	31.5
29000	82.90	1.53×10^8	5.06×10^9	33.1
30500	87.19	2.82×10^8	9.70×10^9	34.4
32000	91.48	5.06×10^8	1.82×10^{10}	36.0
33500	95.77	8.92×10^8	3.32×10^{10}	37.2

[a]The complexes used are the 1.8, .8, .2, .2 bond model (model II).

The same consideration apply for a primary isotope effect. The maximum effect occurs as the sum ratio approaches unity. However, ε_{oH}, is not equal to ε_{oD} as it is in a pure secondary isotope effect, but is smaller. Therefore the sum ratio does not equal unity at any convenient starting point. The maximum effect depends upon the particular system, but occurs at the energy where $\Sigma(P_{\varepsilon V^+})_D$ has overtaken $\Sigma P(\varepsilon V^+)_H$. This energy aspect is thus an additional factor upon the energy level sums and densities and adds to the magnitude of the isotope effect. The total isotope effect in chloroethane elimination reactions is a combination of primary and secondary effects which is of course dependent upon the ε_{oD}, ε_{oH}, and the average energy of both systems.

The pertinent equations for the thermal equilibrium rate constants are

$$k_\infty = \int_{\varepsilon_o}^{\infty} k_\varepsilon \cdot K(\varepsilon) dE = \frac{\sigma kT}{h} \frac{Q_r^+ Q_v^+}{Q_r^* Q_v^*} e^{-\varepsilon_o/RT} \qquad (13)$$

σ is the reaction path degeneracy;

h is the Boltzman constant;

Q_r is the rotational partition function for total rotational degrees of freedom;

Q_v is the total vibrational partition function;

$^+$ refers to complex;

* refers to molecule; and

$K(\varepsilon)$ is the thermal Boltzman distribution

In any real system the molecules are formed with a distribution of energies and those distribution functions must be found.

The thermal distribution function is the quantum Boltzman distribution.

$$K(\varepsilon_{vr})d\varepsilon_{vr} = \frac{N^*(\varepsilon_{vr})\exp[-(\varepsilon_{vr}/\bar{r}T)]d\varepsilon_{vr}}{Z_{vr}^*}$$

Z_{vr}^* is the partition function for all active degrees of freedom of the molecule.

For a chemical activation system in which the energized molecules are formed by the combination of free radicals, the distribution function is given by

$$f(\varepsilon_{vr})d\varepsilon_{vr} = k'_{\varepsilon}K(\varepsilon_{vr})d\varepsilon_{vr} \Big/ \int_{\varepsilon_0'}^{\infty} k'_{\varepsilon}K(\varepsilon_{vr})d\varepsilon_{vr}$$

where the primed terms refer to the reverse of the reaction responsible for the formation of the chemically activated molecule. $K(\varepsilon_{vr})$ is the thermal quantum statistical Boltzman distribution function at the temperature of the formation reaction.

In order to evaluate k'_{ε}, models of the transition state for the radical association reactions must be selected. Such complexes are quite loose and may have free rotation within the complex such as a Gorin model (47) or may alternatively have four very low bending frequency vibrations about the forming bond (2). The latter case was used for these calculations. These complexes essentially consist of CH_3 and CH_2Cl radicals with four added low bending frequencies (Table VIII). The frequencies with the exception of the ν_2 out of plane bend (48) were estimated from

CH_3Cl, CD_3Cl, C_2H_5Cl, and C_2D_5Cl. The CH_2Cl radical fits the Teller-Redlich (49) product rule with the CD_2Cl radical and the CH_3 radical fits the product rule with the CD_3 radical.

A rough test for the model is to consider the equilibrium between $CH_3 + CH_2Cl \underset{k_2}{\overset{k_1}{\rightleftharpoons}} CH_3CH_2Cl$; k_2 calculated from equation 13 at 298 K is 8.71×10^{-9} sec^{-1}. K_{eq} calculated from statistical mechanical considerations (50) of the models for C_2H_5Cl, CH_3 and CH_2Cl is 1.77×10^3 atoms/cc at 298 K. If the bimolecular combination rate constant is represented by a steric factor, P, times the collision rate constant $\sigma^2 (\frac{8\pi kT}{\mu})^{1/2}$, the steric factor should be between 0.1 and 0.01 as is the case for most radical combination reactions. Using 4.2 A for the collision diameters of both CH_3 and CH_2Cl a temperature of 298 K and an electronic steric factor of 2 for each radical gave P = 0.01.

Table VIII. Association complex for chloroethanes.

Mode	C_2H_5Cl complex	C_2D_5Cl complex
CH_3 stretch	3056(3)	2230(3)
CH_3 bend	1400(2)	980(2)
" out of plane bend[a]	730	567
CH_2 stretch	3056(2)	2230(2)
CH_2 bend	1435	980
HC-Cl bend	1000	800
C-Cl stretch	676	615
Out of plane bend	600	427
Low frequency bends	230(2) 150(2)	140(2) 190(2)

[a] Ref. 48.

The 1,2-dichloroethane association complex consists of two groups of CH_2Cl radical frequencies held together by four low frequency bends. The grouped frequencies for the nondeuterated case are 3056(4), 1198(4), 637(4), 178(2), 120(2). The grouped frequencies for the deuterated case are 2230(4), 863(4), 514(4), 106(2), 72(2).

Fig. 6 shows the distribution functions for the chloroethane system. These are important because they are different for the deuterated and nondeuterated cases. Analysis of the nonequilibrium distributions indicates that .55 kcal $mole^{-1}$ difference in the average energy arises from the difference in shape of the curves for the C_2H_5Cl: C_2D_5Cl system; and another 1 kcal $mole^{-1}$ comes from the difference in Emin of the systems. For the $C_2H_4Cl_2$:$C_2D_4Cl_2$ system .45 kcal $mole^{-1}$ comes from the difference in the curves and the remaining .51 kcal $mole^{-1}$ comes from the difference in Emin. For comparison with the nonequilibrium distributions fig. 6 also shows the thermal Boltzman distribution at 720 K.

Thermochemistry. In order to calculate specific rate constants the critical energy ε_o and the minimum energy of the formed molecules, i.e., the start of the distribution function, must be known. A survey of literature has been previously done (1,2) and the same values were adopted for this thesis. They are completely summarized in appendix III. Two new thermal pyrolysis studies have been published (15,16) since the previous literature survey. These now favor Arrhenius parameters of $A = 3.16 \times 10^{13}$ sec^{-1} and $E_a = 56.5$ kcal $mole^{-1}$. These values when put into the

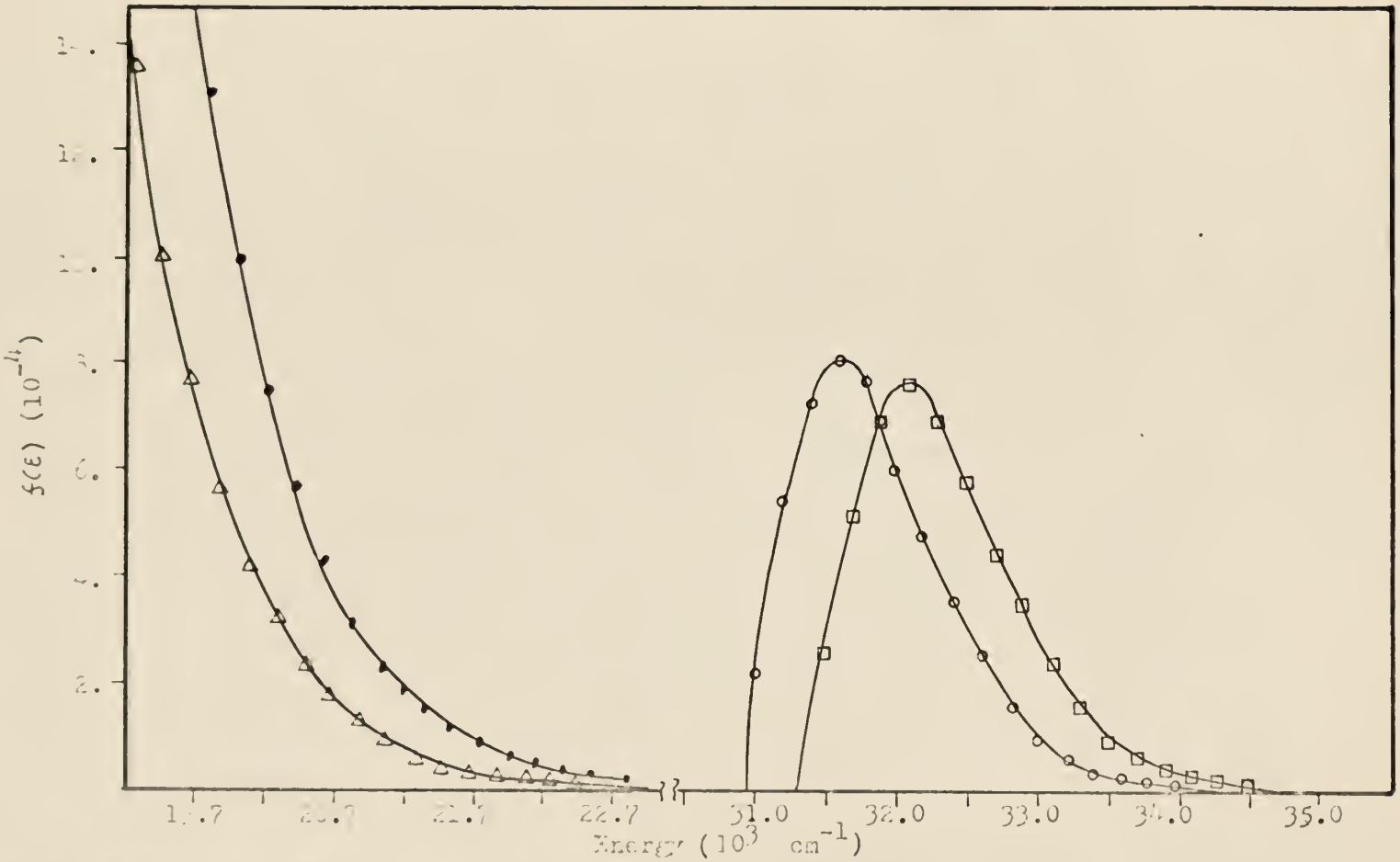

. . Diagrammatic representation of the chloroethane system.
△ = thermal Boltzmann distribution for internal degrees of freedom for C_2H_5Cl at 720 K.
○ = [illegible] activated nonequilibrium distribution function for C_2H_5Cl at 298 K.
□ = [illegible] activated nonequilibrium distribution function for C_2D_5Cl at 298 K.
• = thermal Boltzmann distribution for internal degrees of freedom for C_2D_5Cl at 720 K.

form of equation 13 gives a pre-exponential factor 1.23×10^{13} sec^{-1} at 800 K and an ϵ_o of 55.0 kcal $mole^{-1}$. Conversion to ϵ_o from ϵ_a requires using models of complexes and the molecule. The numbers quoted here are average changes for various models. Hereafter a constant ϵ_o is assumed and small variations then result for ϵ_a. Previously selected values (1,2) were A = $.97 \times 10^{13}$ and the same ϵ_o. The ϵ_o for the isotopic molecules were calculated for each individual case from the zero point energy changes of the models.

The Arrhenius parameters and Emin for 1,2-$C_2H_4Cl_2$ are not known very well and this makes the calculations for it and 1,2-$C_2D_4Cl_2$ less meaningful. An Emin of 85.3 kcal $mole^{-1}$ and the ϵ_o from C_2H_5Cl were used.

Molecule models. A summary of the molecular models is given in Table IX. Frequencies for C_2H_5Cl (51) and $C_2H_4Cl_2$ (52) are available. Frequencies for C_2D_5Cl and $C_2D_4Cl_2$ are not known and were estimated from analogous compounds. The resulting frequencies for C_2D_5Cl compare favorably with those used by Heydtmann and Volker (18). The frequencies chosen in both cases fit the Teller-Redlich (49) product rule to within 10%. The frequencies have been grouped by taking the geometric mean of sets of neighboring frequencies of similar magnitude. The torsional degree of freedom was treated as a vibration for the RRKM formulation. It is possible to treat the torsional degree of freedom as an internal rotation, but a vibrational model has previously (2) been found to be an adequate representation. The overall rotations are considered to be adiabatic. It is possible to estimate the partition

Table IX. Molecular models.

Molecule	Frequencies (cm^{-1})	E_z [d]	Moments of inertia[e] ($amu \cdot A^2$)
C_2H_5Cl[a]	2940(5)	40.10	16.11
	1376(6)		92.19
	1007(3)		101.9
	728(2)		
	336(1)		
	276(1)		
C_2D_5Cl[b]	2160(5)	30.11	24.70
	1059(4)		108.3
	865(5)		120.2
	599(2)		
	300(1)		
	198(1)		
1,2-$C_2H_4Cl_2$[c]	2981(4)	35.23	17.17
	1335(5)		348.7
	1054(3)		359.5
	743(3)		
	300(1)		
	223(1)		
	125(1)		
1,2-$C_2D_4Cl_2$[b]	2190(4)	27.04	26.15
	1010(5)		352.6
	840(3)		366.0
	664(3)		
	276(1)		
	205(1)		
	108(1)		

[a] Ref. 51.

[b] Estimated, see appendix II

[c] Ref. 52.

[d] $E_Z = \sum^{3N-6} 1/2(h\nu)$

[e] Systematically calculated from a computer program and literature values for bond lengths and angles.

function for the hindered internal rotations for the chloroethanes and to use these for calculating the thermal activation high pressure rate constants. A method by Pitzer (53) was used for the calculations using a potential barrier of 3.5 kcal mole^{-1} (2) for the chloroethanes. The potential function for the 1,2-dichloroethanes has a double minimum (54) and does not fit Pitzer's method, so this degree of freedom was simply treated as a vibration.

The moments of inertia were calculated by programming on a 1410 computer. The moments of inertia and structural parameters for C_2H_5Cl are known (55) and the computer program was verified by comparing calculated moments of inertia with experimental values; the agreement was within 1%. For the 1,2-dichloroethanes two CH_2Cl or CD_2Cl sections from the chloroethanes with a C-C bond length of 1.54 A was used to calculate the coordinates of the atoms.

Activated complex. A complete description of the activated complex for the chloroethanes has appeared previously (2). It will be briefly reviewed now for C_2H_5Cl for the readers convenience and details will follow in Appendix II. The activated complex is represented as a near planar four-centered complex as shown below

The reaction proceeds by a simultaneous breaking of bond 2 and bond 4 and the formation of bond 1 and bond 3. The model consists of three distinct parts.

(1). Twelve of the normal modes are out of ring C-H stretches and CH_2 bending vibrations. They were chosen for the most part by analogy with ethene (56).

(2). Five of the normal modes are in-plane ring vibrational frequencies. First bond orders were assigned to bonds being formed or broken, then from Paulings equation (57) the bond lengths were obtained. Force constants for the fractional order bonds were obtained from Paulings form of Badgers rule (57) and a valence force model was used to calculate the frequencies by the Wilson F-G Matrix method (49). The use of Paulings form of Badgers rule is optional and will be analyzed in a forthcoming section (Physical significance of bond order section). The ring bending force constant was arbitrarily set at one tenth the C-H stretching force constant. The varying of the bond orders gives rise to the different models discussed in this thesis. For most cases the total bond order was conserved.

(3). The last normal mode is the out-of-plane ring frequency (puckering). Since there are no stable molecules with a H in the ring to use as an example, it was treated as a "reasonable" adjustable parameter and varied to best fit the experimental kinetic data. From previous results with C_2H_5Cl and C_2H_5Br a value of 400 cm^{-1} had been selected and this was maintained for the non-deuterated molecule. Table X contains a summary of the complexes and frequencies used.

Table X. Models of the four centered activated complex

Model	Bond[a] orders	Bond[a] lengths	Moments of inertia (amu.A^2)	Ring in[b] plane (cm^{-1})	Ring[c] out of plane (cm^{-1})	Out of[d] ring (cm^{-1})	E_Z[e]
I. C_2H_5Cl	1.9,.9, .1,.1	1.35,1.82, 1.99,1.80	18.47 76.70 88.36	1223,608, 751,638, (35)	400	3050(4) 1393(2) 987(4) 890(2)	34.78
Ia. C_2D_5Cl	1.9,.9, .1,.1	1.35,1.82 1.99,1.80	28.87 89.05 104.3	1144,582 539,461 (33)	338	2270(4) 1040(2) 739(4) 632(2)	26.36
II. C_2H_5Cl	1.8,.8, .2,.2	1.37,1.86 1.78,1.59	18.77 75.55 87.51	1177,576, 920,854, (38)	400	3050(4) 1393(2) 987(4) 890(2)	35.21
IIa. C_2D_5Cl	1.8,.8, .2,.2	1.37,1.86, 1.78,1.59	28.65 87.65 102.7	1101,548, 660,618, (35)	330	2270(4) 1040(2) 739(4) 632(2)	26.65
III. C_2H_5Cl	1.5,.5, .5,.5	1.42,2.00, 1.49,1.30	20.52 78.25 91.96	1046,463, 1595,963 (49)	400	3050(4) 1393(2) 987(4) 890(2)	35.99
IIIa.	1.5,.5, .5,.5	1.42,2.00, 1.49,1.30	30.23 90.28 106.9	978,441, 1142,705 (46)	317	2270(4) 1040(2) 739(4) 632(2)	27.10
IV. C_2H_5Cl	1.25,.75, .25,.75	1.48,1.88, 1.71,1.18	20.58 74.69 88.46	937,558, 890,1621, (51)	400	3050(4) 1393(2) 987(4) 890(2)	35.91
IVa. C_2D_5Cl	1.25,.75, .25,.75	1.48,1.88 1.71,1.18	30.23 86.80 103.4	877,530 646,1171, (47)	317	2270(4) 1040(2) 739(4) 632(2)	27.04

Continuation of Table X.

Model	Bond[a] orders	Bond[a] lengths (A)	Moments of inertia (amu.A^2)	Ring in[b] plane (cm^{-1})	Ring[c] out of plane (cm^{-1})	Out of[d] ring (cm^{-1})	E_Z[e]
V. C_2H_5Cl	1.5,.12, .43,.12	1.40,2.19, 2.27,1.49	19.21 103.1 115.5	1046,276, 1319,624, (40)	400	3050(4) 1393(2) 987(4) 890(2)	34.85
Va. C_2D_5Cl	1.5,.12, .43,.12	1.40,2.19, 2.27,1.49	29.32 117.8 133.5	978,263, 944,456, (37)	333	2270(4) 1040(2) 739(4) 632(2)	26.21
VI. $C_2H_4Cl_2$	1.8,.8, .2,.2	1.37,1.86, 1.78,1.59	74.43 160.8 331.9	946,574, 918,835, (28)	400	3100(3) 1400(2) 1000(2) 920(2) 700(2) 400(1)	30.61
VIa. $C_2D_4Cl_2$	1.8,.8, .2,.2	1.37,1.86, 1.78,1.59	84.88 170.2 338.1	896,547, 658,597, (27)	327	2325(3) 1035(2) 750(2) 690(2) 651(2) 340(1)	23.73

[a] The bond orders and bond lengths are listed for the C-C, C-Cl, H-Cl, and H-C bonds, respectively, around the ring of the complex.

[b] Calculated by Wilson F-G matrix method as explained in the text. The frequency in parentheses is the normal mode frequency used for the reaction coordinate.

[c] Assumed values. See appendix II.

[d] Assigned by analogy with ethene, chloroethane, and cyclobutane. See appendix II.

[e] $E_Z = \sum_{1}^{3N-6} 1/2(h\nu)$

The frequencies for the deuterated complex were assigned using the same procedure as for the nondeuterated complex. Since for the out of plane frequencies C_2H_4 was used as the major model for the C_2H_5Cl complex, C_2D_4 (56) was used as the major model for the C_2D_5Cl complex. The ring frequencies were computed from the Wilson F-G matrix method with the appropriate mass changes. The puckering vibration was assigned by treating the 1.8,.8,.2,.2 bond complex as a four membered ring with the corners treated as point masses and fitting the product rule with the nondeuterated complex, assuming 400 cm^{-1} for the nondeuterated complex. The product rule was set 10% high i.e. the deuterated frequencies were set high so that the frequencies ratio was 10% higher than the mass ratio. The complex was finally subjected to the product rule using all the coordinates of the true complex. The product rule was readjusted by varying the out-of-ring frequencies until the frequency ratio of the product rule equation was 10% high. This then set the out-of-plane frequencies for C_2D_5Cl complex. The other bond order models consisted of calculating the ring-in-plane frequencies for the deuterated and nondeuterated complex and assigning the puckering frequencies on the basis of the product rule. See appendix II for a more detailed analysis.

For $C_2H_4Cl_2$, C_2H_3Cl was used as the major contributing model for the out-of-ring vibration. Since C_2D_3Cl frequencies are not known, estimates were made for the out of plane frequencies after considering how particular frequencies changed in other molecules such as the C_2H_5Cl;C_2D_5Cl and $C_2H_2Cl_2$:$C_2D_2Cl_2$ systems. The rest of the frequencies were obtained in the same fashion as described for the chloroethane system.

Comparison of calculated and experimental rate constants. A good model should be able to reproduce the experimental thermal A factor. The calculated A factors are given by $e\frac{kT}{h}\frac{Q^{\ddagger}_{vr}}{Q^{*}_{vr}}$ and are summarized in Table XI for the nondeuterated molecules. An ξ_a can be calculated (58) from ϵ_o and both values are also listed. The ξ_a values have no special significance since the ϵ_o value was chosen on the basis of an average change between ξ_a and ϵ_o for several models of this type. It is seen that models II, III, and IV fit the experimental data fairly well although the A factors are high. Model II (1.8,.8,.2,.2 bond model) is an asymmetric complex in which the C-H and Cl-H bonds are nearly broken. Model III (1.5,.5,.5,.5 bond model) is a symmetric model in which the bond changes are taking place uniformly. Model IV (1.25,.75,.25, .75 bond model) is a slightly summetric model in which the H-Cl bond is weaker than the C-Cl and H-C bonds. Model I (1.9,.9,.9, .1,.1 bond model) is an even more asymmetric bond model than model II. The A factor is sensitive to frequencies below 700 cm^{-1} and in this last case the C-H and H-Cl bonds in the ring were loosened too much and rather low frequencies resulted causing the A factor to be high. Model V is a model developed by Benson and Haugen (59). Their cited bond lengths and bond orders were used with our valence-force method of obtaining frequencies. This is somewhat incorrect because their model contains ionic character but the overall results should be useful. The A factor is much to high. The reasons Model II, III, and IV are much the same is a result of an intricate balancing of the frequencies and moments of inertia changes. Although the low

frequencies are somewhat different, that effect is counterbalanced by bond length which give different changes moments of inertia, e.q. the $Q^{\ddagger}_{vib}$ are 2.14×10^{1} and 2.08×10^{1} and the Q_{rot} are 1.18×10^{5} and 1.29×10^{5} for complex model II and III, respectively.

Table XI. Calculated thermal equilibrium results for C_2H_5Cl and $C_2H_4Cl_2$.

Model[a]	C_2H_5Cl[b]	ε_o[c] kcal mole^{-1}	ε_a kcal mole^{-1}	$C_2H_4Cl_2$[b] A(sec^{-1})	ε_o[c] kcal mole^{-1}	kcal mole^{-1}
Exp	$1.23\ 10^{13}$ [d]	55.0	56.50	$2.46\ 10^{13}$ [e]	55.0	
I	$1.76\ 10^{13}$	55.0	57.03			
II	$1.46\ 10^{13}$	55.0	56.78			
III	$1.54\ 10^{13}$	55.0	56.55			
IV	$1.41\ 10^{13}$	55.0	56.56			
V	$3.53\ 10^{13}$	55.0	57.14			
VI				$2.21\ 10^{13}$	55.0	56.51

[a]The bond orders and frequencies of the models are given in table X.
[b]The calculated Arrhenius A factors are given by $\sigma\frac{kT}{h}\frac{Q^{+}}{Q^{*}}$ and the tabulated values are for 800 K. Proper allowance (a factor of .707) was made for the hindered rotor of C_2H_5Cl but not 1,2-$C_2H_4Cl_2$.
[c]The ε_o values were chosen from experimental Arrhenius activation energies.
[d]Calculated assuming our "best" values chosen from literature.
[e]Estimated value.

The calculated results for k_a are summarized in Table XII for the nondeuterated species. Average energies of the formed chemically activated molecules were obtained from the distribution

function; only the high pressure values are listed in the table because the rate constants show only a small (=4%) change with pressure on a unit deactivation model. A definite improvement in absolute fit occurs in going from the symmetric to assymmetric models. In all models the A factors are too high and the k_a values somewhat too low. For this reason the out-of-ring methylene bending frequencies, which are intermediate in magnitude, were chosen as low as seemed reasonable. Apparently the better simultaneous fit to thermal and chemical activation rate constants is obtained from an assymmetric model; other reasons for favoring an assymmetric model will be developed throughout the rest of the discussion. It should be noted that these models are the result of using Pauling's form of Badger's rule (57). Using a different form of Badger's rule would give a slightly different interpretation of the bond order of the complexes. The trends between assymmetric and symmetric complexes would remain the same however. The calculations for the 1,2-dichloroethanes were only carried out using the asymmetric 1.8,.8,.2,.2 bond order case. Since ϵ_o has been estimated, it is pointless to make detailed analysis for this molecule.

The spirit of approach concerning the calculations is the same as initiated by Hassler (1). However, several small non-critical errors and changes in points of view have been detected and corrected and new calculations for 1,1-$C_2H_4Cl_2$ are done in Appendix V. The original moments of inertia were incorrect due to a systematic error in evaluation of the coordinates of the out-of-ring atoms. The C-C bond length, calculated for a 1.8

Table XII. Calculated rate constants using the RRKM formulation.[a]

Model	C_2H_5Cl $k_a(sec^{-1})$ $\langle\epsilon\rangle^b$ = 91. kcal/mole	$C_2H_4Cl_2$ $k_a(sec^{-1})$ $\langle\epsilon\rangle^b$ = 88 kcal/mole
Exp	4.17×10^9 [c]	1.79×10^8 [c]
I	3.32×10^9	
II	2.46×10^9	
III	2.29×10^9	
IV	2.12×10^9	
V	6.81×10^9	
VI		9.57×10^8

[a] Experimental work and calculations are at 298 K.

[b] Average energy of the formed chemically activated molecules at 298 K.

[c] Corrected for incomplete collisional efficiency by a factor of .9. This factor is a ratio of the rate constants using a collisional deactivation model (described in text) with a jump size of 14.3 kcal $mole^{-1}$ and a unit deactivation model. The value is an average of the ratios for the C_2H_5Cl, C_2D_5Cl, 1,2-$C_2H_4Cl_2$ and 1,2-$C_2D_4Cl_2$ cases.

bond, was originally 1.32 A which was shorter than a double bond. It has now been changed to 1.37 A by using better values in Pauling's equations. Also the calculations in Hassler's thesis (1) were for $\mathscr{P}$ = 3 rather than 2. Finally the ring puckering frequency has been changed from 500 cm^{-1} to 400 cm^{-1}.

Isotope effects. In the previous section comparisons of calculated absolute values of rate constants were made with the experimental absolute values. Relatively good agreement was obtained but there was no clear way to distinguish between several proposed models. In this section the kinetic isotope effects will be used

for this purpose. The calculated values for rate constants from the different models are given in Tables XIII and XIV.

Table XIII. Comparison of calculated and experimental isotope data.

Model	A_H/A_D [a]	ϵ_o [b]	$\frac{k_\infty H}{k_\infty D}$ [c]	$\frac{k_a H}{k_a D}$ [d]
Exp	.57[e]	2.01[e]	1.99[e]	3.33
I	.85	1.57	2.58	3.02
II	.90	1.44	2.49	2.98
III	.98	1.11	2.15	2.84
IV	.97	1.13	2.16	2.82
V	.92	1.36	2.40	3.02

[a] Ratio of A factors at 712 K. A factors are given by $\sigma kT/k\ Q^+/Q^*$

[b] The difference in critical energies $\epsilon_o D - \epsilon_o H$.

[c] k_∞ ratio at 712 K. The average energies of the energized molecules are 56.9 and 58.4 kcal $mole^{-1}$ for C_2H_5Cl and C_2D_5Cl respectively.

[d] k_a (chemical activation) ratio at 298 K.

[e] Experimental values are those of Heydtmann and Volker, ref. 18. His ref 5a was used for the nondeuterated Arrhenius equation. ϵ_o and the corresponding A was calculated by lowering Heydtmanns and Volker's ϵ_a by the same amount to ϵ_o as our 1.8,.8,.2,.2 bond model. This method makes the $\Delta\epsilon_o$ somewhat temperature dependent. It should be noted that the Arrhenius factor ratio given by Heydtmann and Volker, kH/kD = .74 exp 2090/RT and as a consequence the converted form, kH/kD = .57 exp 2010/RT, will not give the exact value of 1.99 they measured at 712.5 K. The Arrhenius form value is 2.37. Using our "best" values for the C_2H_5Cl parameters the entries would be A_H/A_D = .65, $\Delta\epsilon_o$ = 2.065, and $k_\infty H/k_\infty D$ = 2.80.

Table XIV. Summary of calculated kinetic data for C_2D_5Cl and $C_2D_4Cl_2$.

Model	C_2D_5Cl[a] A(sec^{-1}) ([illegible]e-92.6)	ε_o[b] kcal $mole^{-1}$	ε_a[c] kcal $mole^{-1}$	k_{aD}[d] sec^{-1}
Exp_a[f]	1.94×10^{13}	56.90[f]	58.70	1.25×10^{9}
Ia	2.08×10^{13}	56.57	58.58	1.10×10^{9}
IIa	1.63×10^{13}	56.44	58.24	8.26×10^{8}
IIIa	1.58×10^{13}	56.11	57.69	8.06×10^{8}
IVa	1.46×10^{13}	56.13	57.71	7.49×10^{8}
Va	3.85×10^{13}	56.36	58.49	2.25×10^{9}
VIa[g]	2.46×10^{13}	56.30	57.87	3.41×10^{8}

[a] The calculated Arrhenius A factors are given by $\sigma \frac{kT}{h} \frac{Q^{+}}{Q^{*}}$ and the tabulated values are for 800 K. Proper allowance (a factor of .707) was made for the hindered rotor of C_2D_5Cl.

[b] Calculated from ε_{oH} and zero point energies. See appendix II.

[c] Calculated from ε_o. See reference 58.

[d] k_{aD} are at a temperature of .298 K, see footnote c, table XII.

[e] Average energy of the formed chemically activated molecules at 298°K.

[f] Experimental values were calculated from Heydtmann and Volker's Arrhenius equation (18). $k_{\infty} = 6.02 \times 10^{13} \exp - (58700/RT)$, the ε_o was obtained by lowering ε_a the same amount to ε_o as our model II, i. e. 1800 cal/mole.

[g] This model is for $C_2D_4Cl_2$ at 800 K.; K_a at 298°K, $\langle \varepsilon \rangle = 89.25$ kcal/$mole^{-1}$ (average energy of the formed chemically activated molecules at 298°K)

The numerical $\frac{k_\infty H}{k_\infty D}$ values are compared at 712 K with the experimental data obtained by Heydtmann and Volker (18) at the same temperature. The apparent trend for the absolute value of the thermal rate constant ratio seems to favor the symmetric models. However, dividing the experimental data into the appropriate pre-exponential and critical energy differences points to a large $\Delta\varepsilon_o$. A reasonable experimental value for ε_o obtained by lowering Heydtmann and Volker's $\varepsilon_a D$ by the same amount as the 1.8,.8,.2,.2 bond model and subtracting from this value our 55.0 kcal mole^{-1} for the ε_o of C_2H_5Cl chosen as the "best" value from a survey of literature indicates a $\Delta\varepsilon_o$ of 2.06 (see footnote f of Table XIV). Since Blades reports a $\varepsilon_a D - \varepsilon_a H$ value of 2.30 (43) and 2.64 kcal/mole (44) for the $C_2H_5Br:C_2D_5Br$ system at temperatures surrounding 800 K, this large $\Delta\varepsilon_o$ appears to be justified (assuming $\varepsilon_o D - \varepsilon_o H$ and $\varepsilon_a D - \varepsilon_a H$ will not be greatly different). A large $\Delta\varepsilon_o$ would then indicate a preference for the asymmetric models. It appears that in attempting to fit the $\Delta\varepsilon_o$ factor our models may have overestimated the A_H/A_D factor. However, Heydtmanns and Volkers fall-off data ratio does not undergo the customary decline with pressure (see appendix IV) and an error in the k_∞ extrapolation would change the A_H/A_D ratio. Thus, at the present time the large $\Delta\varepsilon_o$ seems to be the most significant criteria.

Since a large $\Delta\varepsilon_o$ has been judged to be important, a problem arises in closely defining this value in our models. Since the $\Delta\varepsilon_o$ was obtained from zero point energies of both the complex and molecule, which depends upon the assigned frequencies, the work is handicapped by not knowing exactly the experimental C_2D_5Cl

molecule frequencies. However, the E_z was identical with Heydtmann and Volker's value which was deduced from unpublished but measured frequencies. If one considers the molecule frequencies as being correct, a large change in the structure of the complex in order to obtain an additional change in ΔE_o of .4 to .5 kcal $mole^{-1}$ would have to occur. For example, the out of plane C-D stretch frequencies of the complex would have to be raised by 35 cm^{-1}. This would make the product rule a factor of 17% high and would make the C-D frequencies unreasonable relative to the C-H frequencies. Since the error limits of Heydtmann and Volker's E_a values are $\pm$.5 kcal $mole^{-1}$, the fit our complexes to the experimental ΔE_o is probably sufficient.

Next consider the nonequilibrium rate ratios $k_\infty H/k_\infty D$. An apparent trend exists which favors the asymmetric over the symmetric bond models. In the previous section it was also noticed the absolute fit for each individual rate constant followed this same trend. The trend is felt to be significant and supports the favoritism for the thermal data for the asymmetric models. Model V is also an asymmetric model and gives good agreement with the isotope effects. It does not fit the absolute values of the rate constants and can be eliminated on that basis.

The pointing of the nonequilibrium results toward an asymmetric model is felt to be significant but the nonequilibrium isotope effect judgments is certainly based on somewhat meager evidence. A mere lowering of the out of plane (puckering) frequencies in the deuterated Model III and Model IV of 6 and 8 cm^{-1}, respectively, will negate the trend. However, Models I

and II would still be favored over either II or III. The sum of states $\Sigma p(\varepsilon_v^+)$ is particularly sensitive to low frequencies and the low ring puckering frequency greatly influences the rate constant. It is difficult to judge whether the $\Sigma p(\varepsilon_v^+)$ or the change in ε_o, which is undergoing a significant increase in going from a symmetric model to an assymmetric model, is most important without detailed calculations which are carried out in Table XV.

An ε_o change corresponding to the difference between a symmetric and asymmetric model would be $\approx$ .3 kcal mole^{-1}. This gives a change in k_ε of $\approx$ 9%. Thus the ε_o appears to be most important. The interplay of $\Sigma p(\varepsilon_v^+)$ effect and ε_o is an unfortunate consequence of the system and makes the nonequilibrium isotope effects not as useful as might be expected for determining structural changes in a reaction.

The difference in Emin has been set at 1 kcal mole^{-1} for the chloroethane system. It is interesting to note what effect this Emin difference together with the average thermal energy difference plays on the rate constant ratio. Table XVI and XVII shows the analysis of the components of the RRKM rate constant ratio in the spirit of equation (12). For convenience it is repeated here

$$\frac{k_\varepsilon H}{k_\varepsilon D} = \frac{k_r H}{k_r D} \left[\frac{\sum_{\varepsilon_{vr}^+=0}^{\varepsilon-\varepsilon_o} {}_r p(\varepsilon_v^+)_H}{\sum_{\varepsilon_{vr}^+=0}^{\varepsilon-\varepsilon_o} {}_r p(\varepsilon_v^+)_D} \right] \left[\frac{N_\varepsilon D^*}{N_\varepsilon H^*} \right] \qquad (12)$$

Table XV. Effects of $\Sigma\rho(\epsilon_v^+)$ and ϵ_o upon the specific rate constant.[a]

Energy				Energy Freq.[b]				
ϵ^*	$\Sigma P(\epsilon_v^+)$	ϵ_o	k_ϵ	ϵ^*		$\Sigma P(\epsilon_v^+)$	ϵ_o	k_ϵ
32366	$3.19\ 10^8$	56.40	$8.12\ 10^8$	32366	330	$3.15\ 10^8$	56.44	$8.01\ 10^8$
32366	$3.29\ 10^8$	56.30	$8.38\ 10^8$	32366	325	$3.19\ 10^8$	56.44	$8.12\ 10^8$
32366	$3.38\ 10^8$	56.20	$8.61\ 10^8$	32366	320	$3.24\ 10^8$	56.44	$8.24\ 10^8$
32366	$3.48\ 10^8$	56.10	$8.87\ 10^8$	32366	315	$3.27\ 10^8$	56.44	$8.34\ 10^8$

[a] The 1.8,.8,.2,.2 bond model C_2D_5Cl was used.
[b] All other frequencies remain the same as Model IIa.

Table XVI. Comparison of the RRKM formulation factors for C_2H_5Cl and C_2D_5Cl.

Energy (cm^{-1})	C_2H_5Cl			C_2D_5Cl			Comparison[a]		
	$\Sigma\rho(\varepsilon_v^+)_H$	$N_\varepsilon^*{}_H$	$k_\varepsilon H$	$\Sigma\rho(\varepsilon_v^+)_D$	$N^*{}_D$	$k_\varepsilon D$	$\frac{\Sigma\rho(\varepsilon_v^+)_H}{\Sigma\rho(\varepsilon_v^+)_D}$	$\frac{N_\varepsilon^*D}{N_\varepsilon^*H}$	$\frac{k_\varepsilon H}{k_\varepsilon D}$
ε^*									
22000	3.78×10^{23}	6.33×10^{67}	3.23×10^{67}	5.10×10^{24}	1.64×10^{88}	1.67×10^{56}	.741	25.84	19.32
24000	8.30×10^{4}	1.68×10^{7}	2.68×10^{8}	2.24×10^{5}	4.70×10^{9}	2.61×10^{7}	.371	27.96	10.25
26000	9.90×10^{5}	4.22×10^{8}	1.27×10^{8}	4.21×10^{6}	1.27×10^{9}	1.78×10^{7}	.235	30.08	7.14
28000	7.88×10^{6}	1.01×10^{8}	4.24×10^{9}	4.71×10^{7}	3.23×10^{9}	7.82×10^{8}	.167	32.03	5.42
30000[b]	4.82×10^{7}	2.31×10^{8}	1.13×10^{9}	3.75×10^{8}	7.83×10^{9}	2.57×10^{8}	.129	33.98	4.42
31825[b]	2.11×10^{7}	4.73×10^{8}	2.42×10^{9}	2.00×10^{8}	1.69×10^{10}	6.34×10^{8}	.106	35.69	3.81
32000	2.41×10^{7}	5.06×10^{8}	2.59×10^{9}	2.32×10^{8}	1.82×10^{10}	6.86×10^{8}	.104	35.86	3.77
32366[c]	3.18×10^{8}	5.82×10^{9}	2.97×10^{9}	3.17×10^{9}	2.11×10^{10}	8.08×10^{9}	.100	36.19	3.67
34000	1.04×10^{8}	1.07×10^{9}	5.24×10^{9}	1.19×10^{9}	4.04×10^{10}	1.58×10^{9}	.087	37.67	3.32
ε^+									
2000	9.40×10^{13}	4.28×10^{67}	1.20×10^{67}	2.78×10^{24}	1.42×10^{88}	1.04×10^{56}	.338	33.07	11.57
4000	2.80×10^{4}	1.16×10^{7}	1.30×10^{7}	1.48×10^{5}	4.10×10^{9}	1.93×10^{7}	.190	35.29	6.76
6000	4.05×10^{5}	2.98×10^{7}	7.36×10^{8}	2.97×10^{6}	1.12×10^{9}	1.43×10^{7}	.136	37.42	5.15
8000	3.68×10^{6}	7.26×10^{8}	2.75×10^{8}	3.49×10^{7}	2.86×10^{9}	6.55×10^{8}	.105	39.45	4.20
10000	2.46×10^{7}	1.69×10^{8}	7.92×10^{9}	2.89×10^{8}	6.98×10^{9}	2.22×10^{8}	.085	41.42	3.57
12000	1.33×10^{7}	3.76×10^{8}	1.91×10^{9}	1.85×10^{8}	1.63×10^{10}	6.08×10^{8}	.072	43.31	3.14
14000	6.01×10^{7}	8.03×10^{8}	4.04×10^{9}	9.66×10^{8}	3.64×10^{10}	1.42×10^{9}	.062	45.34	2.84

[a] Comparison as described by equation 12.
[b] Average energy of C_2H_5Cl system when the proper distribution function is used.
[c] Average energy of C_2D_5Cl system when the proper distribution function is used.

It is noted that the N_{D}^{*}/N_{H}^{*} ratio increases with energy as expected but it is counterbalanced by the $\Sigma p(\varepsilon_v^+)_H/\Sigma p(\varepsilon_v^+)_D$ which decreases much more rapidly. At 31825 cm^{-1}, the average energy of the C_2H_5Cl system, $k_\varepsilon H/k_\varepsilon D = 3.81$. It is only when the k_ε value for the C_2D_5Cl system is raised to its average energy of 32366 cm^{-1} that the true calculated value of 2.98 is determined. Thus the difference in Emin and the individual distribution functions of the system contribute an $\approx$ 30% lowering of the otherwise calculated rate constant. Emin and the distribution functions must be considered real factors and the approximation that deuterated and nondeuterated systems occur at the same average energy is not adequate. It is noted that a change in energy of 2000 cm^{-1} ($\approx$ 5.7 kcal $mole^{-1}$) around the average energy of the C_2H_5Cl system will vary $k_\varepsilon H \approx 2$ and $k_\varepsilon D \approx 2.5$. A change in ε_o of 2000 cm^{-1} causes k_ε to change a factor of 5-6 for C_2H_5Cl and 6-7 for C_2D_5Cl in the energy range around 32,000 cm^{-1}.

It should be emphasized at this point that the conditions used to obtain the $k_\varepsilon H/k_\varepsilon D$ ratio are an intricate set. The molecules product rule is set 10% low, the complex product rule 8-10% high and Emin at 1 kcal $mole^{-1}$. This was done to best fit the kinetic data. For instance the effect of setting the molecule product rule 5% high and lowering the puckering frequency of the deuterated complex to 300 cm^{-1} and raising the C-D stretches from 2270 to 2300 cm^{-1} is a $k_a H/k_a D = 2.43$ which is too low. The effect of arbitrarily raising ε_o of the deuterated Model II 3 kcal $mole^{-1}$ and holding all other factors constant is a $k_a H/k_a D = 4.00$; again emphasizing that ε_o is a major factor. The calculated rate constant ratio for the 1,2-dichloroethane system is lower than for the chloroethane system.

Table XVII. Comparison of the RRKM formulation factors for $C_2H_4Cl_2$ and $C_2D_4Cl_2$.

Energy (cm^{-1})	$C_2H_4Cl_2$			$C_2D_4Cl_2$			Comparison[a]		
	$\Sigma\rho(\varepsilon_v^+)_H$	$N_\varepsilon^*{}_H$	$k_\varepsilon H$	$\Sigma\rho(\varepsilon_v^+)_D$	$N^*{}_D$	$k_\varepsilon D$	$\frac{\Sigma\rho(\varepsilon_v^+)_H}{\Sigma\rho(\varepsilon_v^+)_D}$	$\frac{N_\varepsilon^* D}{N_\varepsilon^* H}$	$\frac{k_\varepsilon H}{k_\varepsilon D}$
ε^*									
22000	9.49×10^{24}	1.61×10^{88}	9.58×10^{57}	1.08×10^{34}	2.28×10^{99}	6.78×10^{46}	.883	14.15	14.12
24000	2.78×10^{45}	4.47×10^{88}	1.01×10^{77}	5.87×10^{46}	6.77×10^{99}	1.25×10^{76}	.474	15.15	8.14
26000	4.00×10^{65}	1.16×10^{99}	5.59×10^{87}	1.31×10^{67}	$1.88\times10^{10\,10}$	1.00×10^{77}	.306	16.12	5.58
28000	3.72×10^{77}	2.88×10^{99}	2.10×10^{88}	1.65×10^{88}	$4.90\times10^{11\,11}$	4.85×10^{88}	.226	17.03	4.34
30000	2.56×10^{77}	6.78×10^{99}	6.15×10^{88}	1.44×10^{88}	$1.21\times10^{11\,11}$	1.71×10^{88}	.178	17.92	3.60
30885[b]	5.58×10^{77}	9.76×10^{99}	9.31×10^{99}	3.42×10^{88}	$1.79\times10^{11\,11}$	2.76×10^{88}	.163	18.37	3.37
31219[c]	7.42×10^{78}	$1.12\times10^{10\,10}$	1.08×10^{99}	4.69×10^{88}	$2.06\times10^{11\,11}$	3.28×10^{88}	.158	18.43	3.29
32000	1.41×10^{88}	$1.53\times10^{10\,10}$	1.50×10^{99}	9.58×10^{88}	$2.87\times10^{11\,11}$	4.81×10^{99}	.147	18.76	3.12
34000	6.56×10^{88}	$3.32\times10^{10\,10}$	3.21×10^{99}	5.20×10^{99}	$6.44\times10^{11\,11}$	1.15×10^{9}	.057	19.37	2.79
ε^+									
2000	1.94×10^{23}	1.08×10^{88}	2.93×10^{57}	4.96×10^{24}	1.91×10^{99}	3.73×10^{46}	.391	17.74	7.85
4000	2.55×10^{35}	3.06×10^{88}	4.56×10^{67}	3.46×10^{46}	$5.73\times10^{10\,10}$	8.70×10^{56}	.248	18.74	5.24
6000	1.55×10^{56}	8.15×10^{99}	3.10×10^{77}	8.38×10^{67}	$1.60\times10^{10\,10}$	7.53×10^{67}	.185	19.69	4.12
8000	1.66×10^{77}	2.05×10^{99}	1.32×10^{88}	1.14×10^{88}	$4.23\times10^{11\,11}$	3.88×10^{88}	.146	20.56	3.40
10000	1.27×10^{77}	$4.92\times10^{10\,10}$	4.19×10^{99}	1.04×10^{88}	$1.06\times10^{11\,11}$	1.42×10^{88}	.122	21.46	2.95
12000	7.55×10^{77}	$1.13\times10^{10\,10}$	1.09×10^{99}	7.21×10^{99}	$2.51\times10^{11\,11}$	4.12×10^{99}	.105	22.59	2.64
14000	3.73×10^{88}	$2.49\times10^{10\,10}$	2.44×10^{99}	4.03×10^{99}	$5.73\times10^{11\,11}$	1.01×10^{10}	.093	23.05	2.41

[a] Comparison as described by equation 12.
[b] Average energy of $C_2H_4Cl_2$ system when the proper distribution function is used.
[c] Average energy of $C_2D_4Cl_2$ system when the proper distribution function is used.

This conflicts with the experimental results and the resolution of this conflict is discussed below. The same trends apply to an analysis of the 1,2-dichloroethane system as seen in table XVIII. The density ratio is a little smaller and the sum ratio a little larger than for the chloroethanes, although when they are combined they tend to compensate, e.g. at 3200 cm^{-1} of energy the $-d_5$ and $-d_4$ rate constant ratios were 3.77 and 3.12 respectively. The average energies of the deuterated and nondeuterated systems are different and this also plays a major role in the calculated rate ratio.

The experimental C_2H_4Cl and $C_2D_4Cl_2$ data indicate both the calculated absolute and calculated ratio values are in error. Since ε_o is not known one first suspects this. The effect of raising ε_o from 55 to 60 kcal $mole^{-1}$ is

$$\frac{k_a H}{k_a D} = \frac{1.99 \times 10^8}{6.21 \times 10^7} = 3.2$$

This is considerably better, fitting the ratio well and individual absolute values of k_a almost exactly. Additional evidence in the study of C_2H_4BrCl (3) has also suggested that 55.0 kcal $mole^{-1}$ is a lower limit to ε_o. However, again the $C_2D_4Cl_2$ frequencies were estimated and this presents a problem in determining the shift in ε_o with deuteration. A better calculation will have to await further experimental data.

In general one must conclude that the thermochemical values (ε_o, Emin, and average energy) molecule frequencies and complex frequencies are a set of conditions that fit the experimental

nonequilibrium isotope effect data and thermal isotope data. Although there are certain tendencies toward an asymmetric complex in both thermal and nonequilibrium isotope effect data they are by no means conclusive. It appears that these kinds of data are not sufficient to define a best model. Next intermolecular isotope effects will be discussed in order to further decide on a model.

Intramolecular isotope effect. The intramolecular isotope effect is another way of testing the different models. In fact is will be shown that this effect leads to more conclusive evidence in favor of the asymmetric complex. The only intramolecular isotope effect data for the chloroethanes is the pyrolysis of CHD_2-CD_3Cl by Blades (17). The models for the complexes and molecules for this molecule and also C_2H_4DCl will be developed below.

Blade's experimental rate constant was kH/kD = 1.16 $e^{985\pm50}$ which has the value of 2.01 at 900 K. Models for this reaction were created as described earlier. Ethylene-d_0 and d_4 were the chief benefactors to the out of ring frequencies. The ring frequencies were calculated by the Wilson F-G matrix method using the 1.8, 8, -,.2 and 1 5, 5,.5, 5 force bond models with the masses of the atoms changed to correspond to isotopic substitution. The out of plane ring vibrations were set at the same frequencies as the C_2H_5Cl and C_2D_5Cl complexes i.e. for the 1.8, 8,.2,.2 bond model HCl split out, 400 cm^{-1}, DCl split out 330 cm^{-1}. This was justified because the product rule compared with the C_2H_5Cl complex, using only ring frequencies and masses, predicted no change of any significance. When all the frequencies were considered, the product rule was fit, if need be, by varying

out of ring frequencies. The molecules were formed by analogy with known deuterated molecule frequencies as described previously. Exactly the same considerations as described above also apply to the C_2H_4DCl molecule and complexes and the pertinent data are listed in Table XVIII.

The calculated rate constant ratio using the 1.8,.8,.2,.2 bond model is

$$\frac{kH}{kD} = .89\ e^{1065/kT} = 1.61$$

The ε_a compare well, but the agreement between factor ratios are not as good as desired. It is hard to see from the Absolute Rate theory point of view how the A factor ratio can be greater than unity. This point was thoroughly discussed in previous work (1) and it was concluded that the ε_a factor should be a good number because it is not as pressure dependent as the A factor where an error could more easily occur. If one now compares the 1.5,.5, .5,.5 bond model at 900 K:

$$\frac{kH}{kD} = .91\ e^{783/RT} = 1.41$$

The isotope effect is too small and the ε_o difference also too small. We conclude that the 1.8,.8,.2,.2 bond model is the favored one to explain the data.

It is of interest to note that if one compares the k_ε for HCl and DCl nonequilibrium intramolecular elimination from C_2H_4DCl in table XIX at 31825 cm^{-1}, the values are 8.6×10^8 and 7.9×10^8 sec^{-1} respectively. This would give a $k_\varepsilon H/k_\varepsilon D$ ratio of 1.1. This ratio is not large enough for the reaction to be used as an experimental test for further elucidation of the complex. If one now considers the HCl and DCl elimination from C_2D_4HCl (table XX) in the same manner the ratio is 1.2. This molecule is also unfavorable for a possible experimental intramolecular test of the models.

Table XVIII. Data for C_2D_4HCl and C_2H_4DCl molecules and complexes.

Type	Frequencies (cm^{-1})	ε_z kcal $mole^{-1}$	ε_o[a] kcal $mole^{-1}$	Moments of inertia (amu·A^2)
C_2D_4HCl molecule	2160(4),2940(1),1096(6), 848(3),610(2),306(1), 206(1)	32.08		22.84 104.9 116.9
C_2D_4HCl complex HCl^4 split out 1.8,.8,.2,.2	2270(4),1060(3),885(2), 739(4),632(2),549(1), 400(1)	27.45	55.27	26.61 87.62 100.6
C_2D_4HCl complex DCl^4 split out 1.8,.8,.2,.2	3050(1),2270(3),1148(3), 812(3),670(5),548(1), 330(1)	28.55	56.37	27.28 82.80 98.66
C_2D_4HCl complex HCl^4 split out 1.5,.5,.5,.5	2270(4),1040(2),1593(1), 968(2),739(4),632(2), 442(1),400(1)	28.24	55.28	29.16 90.25 105.8
C_2D_4HCl complex DCl^4 split out 1.5,.5,.5,.5	3050(1),2270(3),1156(3), 956(2),715(6),441(1), 330(1)	29.01	56.05	28.56 85.83 102.9
C_2H_4DCl molecule	2940(4),2160(1),1320(6), 967(3),676(2),320(1), 259(1)	38.14		17.85 95.52 105.8
C_2H_4DCl complex HCl^4 split out 1.8,.8,.2,.2	3050(3),2270(1),1280(3), 966(4),812(4),575(1), 400(1)	33.39	55.14	20.09 80.04 92.27
C_2H_4DCl complex DCl^4 split out 1.8,.8,.2,.2	3050(4), 1316(3),987(4), 890(2),642(2),574(1), 330(1)	34.41	56.17	20.76 75.60 89.55

[a]Calculated by vibrational analysis. See equation in appendix II.

Primary and secondary nonequilibrium isotope effects. The object of this section is to speculate on the role of the primary and secondary isotope effects in the calculated experimental rate constant. The frequencies of the molecules and complexes and other pertinent data are given in Table XXIII. First HCl and DCl

Table XIX. Comparison of the RRKM formulation factors for DCl and HCl split out from C_2H_4DCl. Rate constants are per H or D atom.

Energy (cm^{-1})	HCl split out			DCl split out		
ε^*	$\Sigma p(\varepsilon_v^+)$	N_ε^*	k_ε	$\Sigma p(\varepsilon_v^+)$	N_ε^*	k_ε
22000	4.8×10^{2}	1.2×10^{7}	1.0×10^{6}	2.7×10^{2}	1.2×10^{7}	5.4×10^{5}
24000	1.1×10^{4}	3.3×10^{7}	8.6×10^{6}	8.2×10^{4}	3.3×10^{7}	6.5×10^{6}
26000	1.4×10^{5}	8.4×10^{7}	4.3×10^{7}	9.8×10^{4}	8.3×10^{7}	3.2×10^{7}
28000	1.1×10^{6}	2.0×10^{8}	1.5×10^{8}	9.3×10^{5}	2.0×10^{8}	1.2×10^{8}
30000	7.1×10^{6}	4.7×10^{8}	4.0×10^{8}	6.1×10^{6}	4.7×10^{8}	3.5×10^{8}
31825[a]	3.12×10^{7}	9.59×10^{8}	8.57×10^{8}	2.87×10^{7}	9.64×10^{8}	7.93×10^{8}
32000	3.6×10^{7}	1.0×10^{9}	9.2×10^{8}	3.3×10^{7}	1.0×10^{9}	8.5×10^{8}
32366[b]	4.91×10^{7}	1.19×10^{9}	1.04×10^{9}	4.30×10^{7}	1.18×10^{9}	9.81×10^{8}

[a]Average energy of C_2H_5Cl system.
[b]Average energy of C_2D_5Cl system.

Table XX. Comparison of the RRKM formulation factors for DCl and HCl split out from C_2D_4HCl; rate constants are per H or D atom.

Energy (cm^{-1})	HCl split out			DCl split out		
ε^*	$\Sigma p(\varepsilon_v^+)$	N_ε^*	k_ε	$\Sigma p(\varepsilon_v^+)$	N_ε^*	k_ε
22000	8.2×10^{2}	8.7×10^{7}	2.5×10^{5}	6.0×10^{2}	8.8×10^{7}	1.7×10^{5}
24000	2.8×10^{4}	2.5×10^{8}	3.0×10^{6}	2.0×10^{4}	2.5×10^{8}	2.1×10^{6}
26000	4.4×10^{5}	6.6×10^{8}	1.8×10^{7}	3.1×10^{5}	6.5×10^{8}	1.3×10^{7}
28000	4.4×10^{6}	1.7×10^{9}	7.0×10^{7}	3.3×10^{6}	1.6×10^{9}	5.3×10^{7}
30000	3.1×10^{7}	4.1×10^{9}	2.1×10^{8}	2.5×10^{7}	4.0×10^{9}	1.7×10^{8}
31825[a]	1.54×10^{8}	8.41×10^{9}	4.89×10^{8}	1.30×10^{8}	8.43×10^{9}	4.05×10^{8}
32000	1.8×10^{8}	9.0×10^{9}	5.4×10^{8}	1.5×10^{8}	9.1×10^{9}	4.4×10^{8}
32366[b]	2.45×10^{8}	1.05×10^{10}	6.29×10^{8}	2.00×10^{8}	1.04×10^{10}	5.40×10^{8}

[a]Average energy of C_2H_5Cl system.
[b]Average energy of C_2D_5Cl system.

elimination from C_2H_4DCl will be compared to HCl elimination from C_2H_5Cl. If one considers HCl elimination from the C_2H_4DCl, the isotope effect should be nearly a pure secondary effect because the D is not involved in the reaction coordinate; DCl elimination should be a pure primary effect since it is the only isotopically substituted atom and it is in the reaction coordinate. A 1.8,.8, .2,.2 bond complex model was used as a good representative of an asymmetric complex (see physical significance of bond order section) in the following calculations. The comparisons in the tables are at the same total energy. The ε_o is equal to 56.17 kcal $mole^{-1}$. A secondary effect is sometimes defined as pure when the critical energies of the two compared systems are identical. For such a definition, HCl elimination from C_2H_4DCl is not quite pure because the pertinent critical energies are 55 and 55.14 kcal $mole^{-1}$. The k_ε are given in tables XX and XX for the comparison with the C_2H_5Cl system. For the present purposes it is not necessary to find Emin and $f(\varepsilon)$, the rate constants will just be compared directly at the appropriate energies.

For the secondary effect if the k_ε for HCl elimination from C_2H_4DCl at 31825 cm^{-1} (average energy of the C_2H_5Cl system) is compared to k_ε for C_2H_5Cl at 31825 cm^{-1} the ratio is 1.41. For the pure primary effect at 31825 cm^{-1}, the k_ε for DCl elimination from C_2H_4DCl is compared to HCl elimination from C_2H_5Cl. The ratio is 1.53. The secondary effect with four deuterium atoms would be the comparison of the k_ε for HCl elimination from C_2D_4HCl to HCl elimination from C_2H_5Cl.. At 31825 cm^{-1} such a ratio is 2.42 or 1.25 on a per atom basis. There is an ε_o of

55.27 kcal mole^{-1} associated with the C_2D_4HCl reaction. Since this is larger than the ϵ_o for HCl elimination from C_2H_4DCl the secondary effect is dependent upon the ϵ_o and is not "pure". This raising of ϵ_o accounts for part of the difference in the two numerical values of the secondary effect; a part of the difference may also be due to small nonlinear changes of frequency patterns with increasing deuteration.

If one attempts to compare isotope effects of HCl elimination from C_2H_5Cl to DCl elimination from C_2D_5Cl the problem arises that the two systems are at different average energies and have different ϵ_o. Thus, the primary isotope effect ratio for the calculated experimental system is given by the k_ϵ for HCl elimination from C_2H_5Cl at 31825 cm^{-1} divided by the k_ϵ for DCl elimination from C_2H_4DCl at 32366 cm^{-1}, the average energy of the C_2D_5Cl system. This gives a ratio of 1.23. The effect due to the out of ring isotopically substituted atoms would be the remainder of the total calculated rate constant or 2.42. Since there are four deuterium substituents, this is a k_aH/k_aD ratio of 1.25 per atom. The $k_\epsilon H/k_\epsilon HCl$ ratio of 1.41 calculated earlier for a nearly pure secondary effect was obtained by comparing k_ϵ at the same energy. The ratio of 1.25 has taken into account the difference in the average energies of the C_2H_5Cl and C_2D_5Cl systems and nonlinear changes of frequency patterns with increasing deuteration and also the change in ϵ_o associated with this effect. The ϵ_o for the secondary effects for the C_2H_5Cl and C_2D_5Cl cannot be separated from the ϵ_o due to the primary effect, but the difference in ϵ_o for HCl elimination from C_2H_4DCl and C_2D_4HCl

(secondary effect) is .13 kcal mole^{-1} and the C_2H_5Cl and C_2D_5Cl system should have a comparable value. These calculations were made on the assumption that 2.98, the calculated ratio is correct. If one wished to compare to the true experimental system, the relative contributions to the ratio should be good; however, the absolute values are a little low.

Physical significance of bond order. At least thirty different empirical relations have been proposed to relate force constants with molecular parameters (60). One of the simplest describes the variation of harmonic bond stretching force constants with bond length and this correlation is commonly called Badger's rule (61), whether or not one used Badger's original correlation function (60). The Pauling (57) form of Badger's rule, used in this thesis to obtain fractional bond stretching force constants, will in this section be compared to forms of Badger's rule given by Herschbach and Laurie (62) and by H. S. Johnston (63). Since fractional bond force constants are speculative, especially at the small bond orders, the comparisons must necessarily be assumptive.

The bond lengths for fractional bond orders were obtained from Pauling's correlation of bond order and bond length (57)

$$D = D_0 - .71 \log n$$

where D_0 is the single bond length, n is the bond order and D is the bond length corresponding to the bond order in question. The single order bond lengths that were used are 1.55 A for C-C, 1.79 A for C-Cl, 1.28 A for Cl-H, and 1.09 A for H-C. The fractional

order bond lengths were combined with the following Badger's rule equations and the resulting force constants are compared in Table XXI:

A.

$$f = \left(\frac{1}{a(d-b)}\right)^3 \times 10^6 \text{ dynes cm}^{-1}$$

where d = bond length and a and b are the constants. This is the Badger's rule equation given by Pauling. (57).

bond	a	b
C-C	1.75	0.68
C-Cl	1.87	0.94
Cl-H	2.32	0.585
H-C	2.32	0.335

B.

$$f = \left(\frac{a-b}{d-b}\right)^3 \times 10^5 \text{ dynes cm}^{-1}$$

where d = bond length and a and b are the constants. This form was given by Hershbach and Laurie (62) and is an improved version of equation A

bond	a	b
C-C	1.91	0.68
C-Cl	2.28	0.74
Cl-H	1.84	0.38
H-C	1.66	0.30

C.

$$\log f = \left(\frac{a-d}{b}\right) \times 10^5 \text{ dynes cm}^{-1}$$

where d = bond length and a and b are the constants. This form was suggested by Herschbach and Laurie (62) to fit quadratic,

cubic, and quartic force constants.

bond	a	b
C-C	1.73	0.47
C-Cl	2.02	0.53
Cl-H	1.80	0.69
H-C	1.54	0.64

D.

$$\log f = \left(\frac{a-d}{b}\right) \times 10^5 \text{ dynes cm}^{-1}$$

where d = bond length and a and b are the constants. This is the same form as equation C. However, H. S. Johnston (63) has considered the weak bonding in Lennard Jones, noble-gas, two-atom clusters and redefined the constants for this equation to include these weak bonds as well as the usual strong bonds.

bond	a	b
C-C	1.85	0.55
C-Cl	2.06	0.63
Cl-H	1.74	0.64
H-C	1.46	0.56

The equations must at least give back the correct force constant of known single and double bond stretching motions. Also, since in the activated complexes very small bond orders are often used, it appears desirable that the equations extrapolate in a reasonable way to zero values of the force constant at zero bond order. The four Badger's rule equations will be judged upon these two criteria.

If one considers the first criteria, it is clear that equations B, C, and D are superior to equation A in predicting the H-Cl and C-H force constants at a bond order of unity This is a

Table XXI. Comparison of force constants.

Bond	Bond Order	A[b]	B[a]	C[a]	D[a]	Exp[b]
		All force constant units are in dynes cm^{-1}				
C-C	1.0	2.84×10^5	2.83×10^5	2.42×10^5	3.51×10^5	3.36×10^5
	1.5	4.51×10^5	4.50×10^5	4.35×10^5	5.80×10^5	
	1.8	5.71×10^5	5.69×10^5	5.83×10^5	7.46×10^5	
	2.0	6.49×10^5	6.48×10^5	6.76×10^5	8.46×10^5	9.32×10^5
C-Cl	1.0	2.49×10^5	3.15×10^5	2.72×10^5	2.68×10^5	2.42×10^5
	0.8	1.97×10^5	2.61×10^5	2.00×10^5	2.08×10^5	
	0.5	1.27×10^5	1.81×10^5	1.09×10^5	1.25×10^5	
	0.2	6.21×10^4	9.81×10^4	3.10×10^4	4.31×10^4	
	0.1	4.03×10^4	6.70×10^4	1.24×10^4	2.00×10^4	
	.001	5.77×10^3	1.14×10^4	2.60×10^1	1.12×10^2	
H-Cl	1.0	2.39×10^5	4.27×10^5	5.67×10^5	5.23×10^5	4.78×10^5
	0.8	1.79×10^5	3.41×10^5	4.49×10^5	4.07×10^5	
	0.5	1.07×10^5	2.25×10^5	2.81×10^5	2.46×10^5	
	0.2	4.74×10^4	1.14×10^5	1.07×10^5	8.66×10^4	
	0.1	2.89×10^4	7.46×10^4	5.30×10^4	4.07×10^4	
	0.001	3.55×10^3	1.12×10^4	4.64×10^2	2.45×10^2	
C-H	1.0	1.86×10^5	5.10×10^5	5.05×10^5	4.58×10^5	4.71×10^5
	0.8	1.43×10^5	3.95×10^5	3.93×10^5	3.43×10^5	
	0.5	8.81×10^4	2.49×10^5	2.37×10^5	1.93×10^5	
	0.2	4.09×10^4	1.18×10^5	8.35×10^4	5.86×10^4	
	0.1	2.55×10^4	7.46×10^4	3.92×10^4	2.47×10^4	
	0.001	3.33×10^3	1.01×10^4	2.37×10^2	1.39×10^1	

[a] Corresponding equations given in text

[b] Calculated from $\nu = 1/2\pi\sqrt{k}$ using the molecules C_2H_5Cl, C_2H_4 and HCl. Anharmonic corrections were not considered.

result of Herschbach and Laurie's revision of the original Badger's rule constants. The C-Cl and C-C bond stretches are fixed by all forms reasonably well. The second criteria indicates that equations C and D are superior to A and B in predicting a 0 force constant at 0 bond order (.001 bond order is used to simulate 0 bond order). Equation D appears to be the best way to find force constants from bond order.

The fact that equation A, which was used for the calculations in this thesis, was less satisfactory that equation D was not discovered until after most of the calculations were completed. There is no doubt that the asymmetric complex (weak bonds between C-H and Cl-H) is necessary to explain existing data. The problem that now remains is to reinterpret the physical structure of the complex if equation D is considered the better Badger's rule equation. The H-Cl and C-H force constants turn out to be the critical ones since the force constants of the C-C and C-Cl are those for bonds near 1.0 order and since all four equations yield about the same force constants. An examination of the intermediate bond orders and force constants in Table XXI show that actually equation D and equation A predict nearly the same force constants for the 0.2-0.1 bond orders for the H-Cl and C-H cases.

The results of pertinent rate constant calculations will be considered next. Case A designates the calculations previously tabulated in the comparison of calculated and experimental rate constants section. Case B, C, and D designate the results obtained from the other three Badger's rule force constant equations. Table XXII is a summary of the ring frequencies calculated

from a Wilson F-G matrix using equations A, C, and D to obtain the force constants needed. Table XXIII is a summary of the calculated rate constants at 800 K and shows that due to the higher in-plane ring frequencies for the same bond order, for the same bond order specification, case B and D have the effect of lowering the Arrhenius factor and k_a values relative to case A. Table XXIV is a summary of the isotope effects at 712 K and clearly emphasizes the total effect of varying the force constants. The large $\Delta\varepsilon$ that has previously been decided as important (see comparison of calculated and experimental rate constants section) is only achieved by case A, 1.8,.8,.2,.2 bond model, case A, 1.9,.9, .1,.1 bond model, and case D 1.9,.9,.1,.1 bond model; all of which are asymmetric cases. Case A, 1.8,.8,.2,.2 bond model and case D, 1.9,.9,.1,.1 give nearly identical values for the tabulated values in the table. One must conclude that the 1.8,.8,.2,.2 bond model based upon equation A, used in this thesis is equivalent to a 1.9,.9,.1,.1 bond model if equation D is used for the force constants. Use of equation B or C nad forcing agreement with experiment would not conserve bond order because to obtain frequencies for the deuterated and nondeuterated complexes that would give a large $\Delta\varepsilon_o$ by equations B and C would require low bond order specifications all around the ring. The conclusion does not alter any of teh trends stated in this thesis but merely makes the complexes somewhat more asymmetric than before and makes firm statements about bond orders and conservation of bond order between C_2H_5Cl and its complex difficult.

Table XXII. The four centered complex in-plane ring frequencies.[a,b]

Model	Bond Order	Ring in Plane C_2H_5Cl	Model	Ring in Plane C_2D_5Cl
Case A	1.8,.8,. .2,.2	1177, 576, 920, 854, (38)		1101, 548, 660, 618, (35)
Case B	1.8,.8, .2,.2	1175, 662, 1398, 1482, (38)		1104, 631, 1004, 1067, (35)
Case D	1.8,.8, .2,.2	1349, 592, 1243, 1036, (38)		1261, 565, 891, 750, (35)
Case A	1.9,.9,	1223, 608, 751, 638, (35)		1144, 582, 539, 461, (33)
Case B	1.9,.9, .1,.1	1215, 691, 1249, 1057, (35)		1144, 659, 765, 892, (33)
Case D	1.9,.9, .1,.1	1398, 629, 861, 650, (35)		1308, 598, 620, 471, (33)

[a]The bond orders, bond lengths, moments of inertia, ring out of plane freq, and ring out of ring frequencies are the same as in Table X.

[b]Case C is intermediate between case B and D.

Table XXIII. Calculated rate constants.

Model	Bond order	A(sec^{-1}) [a] 800°K	ϵ_o	ϵ_a [b] 800°K	k_a [c] 298°K
Exp [d] C_2H_5Cl		1.23×10^{13}	55.00	56.50	4.17×10^{9}
Exp [d] C_2D_5Cl		1.94×10^{13}	56.90	58.70	1.25×10^{9}
C_2H_5Cl Eq. 2 A	1.8,.8, .2,.2	1.46×10^{13}	55.00	56.78	2.46×10^{9}
C_2D_5Cl Eq. 2 A	1.8,.8, .2,.2	1.63×10^{13}	56.44	58.24	8.26×10^{8}
C_2H_5Cl Eq. 5 B	1.8,.8, .2,.2	1.00×10^{13}	55.00	56.08	1.20×10^{9}
C_2D_5Cl Dq. 2 B	1.8,.8, .2,.2	$.98 \times 10^{13}$	56.00	57.11	4.26×10^{8}
C_2H_5Cl Eq. 5 D	1.8,.8, .2,.2	1.17×10^{13}	55.00	56.36	1.61×10^{9}
C_2D_5Cl Eq. 2 D	1.8,.8, .2,.2	1.21×10^{13}	56.19	57.58	5.57×10^{8}
C_2H_5Cl Eq. 2 A	1.9,.9, .1,.1	1.76×10^{13}	55.00	57.03	3.32×10^{9}
C_2D_5Cl Eq. 2 A	1.9,.9, .1,.1	2.08×10^{13}	56.57	58.58	1.10×10^{9}
C_2H_5Cl Eq. 2 B	1.9,.9 .1,.1	1.09×10^{13}	55.00	56.32	1.50×10^{9}
C_2D_5Cl Eq. 2 B	1.9,.9, .1,.1	1.12×10^{13}	56.22	57.57	5.16×10^{8}
C_2H_5Cl Eq. 2 D	1.9,.9, .1,.1	1.56×10^{13}	55.00	56.83	2.68×10^{9}
C_2D_5Cl Eq. 2 D	1.9,.9, .1,.1	1.75×10^{13}	56.48	58.29	8.94×10^{8}

[a] Corrected by a factor of .707 for hindered rotation the values are for 800°K.
[b] Calculated from ϵ_o. See ref. 58.
[c] K_a values at 298°K.
[d] See tables in comparison of calculated and experimental rate constants section for details.

Table XXIV. Comparison of isotope effects.

Model	Bond order	A_H/A_D [a] 712 K	$\Delta\varepsilon_o$ [b] 712 K	$k_\infty H/k_\infty D$ 712 K	$k_a H/k_a D$ 298 K
C_2H_5Cl Exp [c]		.57	2.01	1.99	3.33
C_2H_5Cl Eq. A	1.8,.8, .2,.2	.90	1.44	2.49	2.98
C_2H_5Cl Eq. B	1.8,18, .2,.2	.97	1.00	2.08	2.81
C_2H_5Cl Eq. D	1.8,.8, .2,.2	.97	1.19	2.26	2.88
C_2H_5Cl Eq. A	1.9,.9, .1,.1	.85	1.57	2.58	3.02
C_2H_5Cl Eq. B	1.9,.9, .1,.1	.99	1.22	2.33	2.90
C_2H_5Cl Eq. D	1.9,.9, .1,.1	.89	1.48	2.54	2.99

[a] A factors given by $\sigma kT/k\ Q^+/Q^*$
[b] The difference in critical energies $\varepsilon_o D - \varepsilon_o H$
[c] See Table XIII.

C_2D_5 and C_2H_5Cl torsional frequencies. After the calculations were completed, K. D. Moller and L. H. London (64) published the CD_3CD_2Cl torsion frequency and a remeasurement of the CH_3CH_2Cl torsion frequency. They found 251 cm^{-1} for C_2H_5Cl and 184 cm^{-1} for C_2D_5Cl. These are lower than the 276 cm^{-1} and 198 cm^{-1} used for C_2H_5Cl and C_2D_5Cl, respectively, in this thesis. The density of states N* for these molecules with the new torsional frequencies were calculated to estimate the effect this would have on the ratio constant. The comparisons are as follows: for C_2H_5Cl at 31159 cm^{-1} the N* was 3.998 10^8 compared to 3.653 10^8 before. For C_2D_5Cl at 31409 cm^{-1} the N* was 1.429 x 10^{10} compared to 1.502 10^{10} before. This constitutes a 7-9% increase in the N* and would be expected to decrease the k_a values by about this amount. The k_a ratios should be little effected.

Conclusion. The experimental k_aH/k_aD ratio for the C_2H_5Cl: C_2D_5Cl and 1,2-$C_2H_4Cl_2$-1,2-$C_2D_4Cl_2$ systems have been successfully interpreted using the RRKM theory. Since one of the main purposes of the calculations was to descern trends and ascertain which type of model would best fit the kinetic data, they were carried out with regard to thermal, intermolecular, and intramolecular kinetic effects. The results appear to indicate that the nonequilibrium intermolecular isotope effect is less sensitive than one would hope in descerning the best models. In order to select the best models it was necessary to study many interacting trends. Despite these difficulties the calculated chemical activation results, calculated thermal pyrolysis results, and the intramolecular pyrolysis isotope effects for C_2D_4HCl

establish an asymmetric bond model, i.e. one with the H loosely bound in the four-centered complex. The exact physical interpretation of the degree of bond rupture or formulation complex was difficult because bond orders specifications are dependent upon the form of Badger's rule used to calculate the force constants for the ring stretching motions. This also make firm statements about the conservation of bond order difficult. However, all considerations seem to favor asymmetric model, i.e. one with weak bonds between the carbon-hydrogen, chlorine and stronger bonds between carbon-carbon and carbon chloride.

APPENDIX I
RRKM Theory

The Rice-Ramsberger-Kassel-Marcus theory is derived in references 4,5,6. The specific rate constant is given by

$$k_\varepsilon = \frac{\sigma}{h}\,\frac{Z_1^+}{Z_1^*}\,\frac{\sum P(\varepsilon_{vr})}{N^*(\varepsilon_{vr})}$$

where the symbols have been defined in the text. For most unimolecular reactions all vibrational degrees of freedom are considered as active and overall rotations are treated as adiabatic; the chloroethanes are treated this way.

The expressions* for $\Sigma P(\varepsilon_{vr}^+)$ and $N\varepsilon_{vr}^*$ are

$$P(\varepsilon_{vr}^+) = \begin{cases} \dfrac{Z_r^+}{(kT)^{r^+/2}\,\Gamma(1+r^+/2)} \displaystyle\sum_{\varepsilon_v^+=0}^{\varepsilon^*} P(\varepsilon_v^+)(\varepsilon^+-\varepsilon_v^+)^{r^+/2}; & r^+\neq 0 \\ \displaystyle\sum_{\varepsilon_v^+=0}^{\varepsilon^+} P(\varepsilon_v^+) & ; \; r^+=0 \end{cases}$$

$$N_\varepsilon^* = \begin{cases} \dfrac{Z_r^*}{(kT)^{r^*/2}\,\Gamma(r^*/2)} \displaystyle\sum_{\varepsilon=0}^{\varepsilon} P(\varepsilon_{vr}^*)(\varepsilon-\varepsilon_v)^{r^*/2-1} & ; \; r^*\neq 0 \\ \dfrac{\partial}{\partial\varepsilon}\left(\displaystyle\sum_{\varepsilon=0}^{\varepsilon} P(\varepsilon_v^*)\right)_{\varepsilon_v=\varepsilon} & ; \; r^*=0 \end{cases}$$

*All terms have been previously defined (38). The $\Sigma P(\varepsilon_{vr})$ was done on an IBM 1410 or 360 computer using the Haarhoff approximation (65) at higher energies and the direct sum method of Harrington (66) at low eneriges. The Haarhoff approximation can also be used to calculate the density of states at higher energies.

APPENDIX II

Procedure for Selection of Models

The frequencies of C_2H_5Cl (51) and $C_2H_4Cl_2$ (52) are known. However, there are no published values for C_2D_5Cl and $C_2D_4Cl_2$ and they were estimated* from the frequencies of CH_3CH_3 and CD_3CD_3. The grouped frequencies were then altered somewhat to fit the Teller-Redlich (49) product rule to within 10%**. The same procedure was followed for $C_2D_4Cl_2$. C_2H_4 and C_2D_4 (56) frequencies were used for comparison in this case. The resulting frequencies are given in Table IX. Heydtmann and Volker (18) have indicated measured but unpublished frequencies for C_2D_5Cl. The frequencies compared favorably with ours.

The frequencies for the activated complexes may be divided into three groups. They are as follows:

(1) Out-of-ring vibrational frequencies. There are a total of 12 of these ring frequencies. Once chosen these frequencies were not varied so they were not treated as parameters. For chloroethane, ethene (56) was chosen as a model to estimate the frequencies of the complex. The deuterated frequencies were obtained analogously by using C_2D_4 as the model. The results are given in Table XXV. For 1,2-dichloroethane, vinyl chloride was used as a model. The deuterated frequencies were estimated in this case. The results are given in Table XXVI.

---

*Fundamental frequencies were used in all cases in this thesis
**It was set 10% low (deuterated frequencies lower than normal) to best fit the kinetic data

Table XXV. Out of plane frequencies for the C_2H_5Cl and C_2D_5Cl activated complex.

Mode	Molecule[b] C_2H_4	Complex nondeuterated
C-H stretch	3056(4)	3050(4)
CH_2 def.	1393(2)	1393(2)
twist	1027(1)	1027(2)
CH_2 wag	948(2)	948(2)
CH_2 rock	1236 810	890(2)[c]
	C_2D_4	Deuterated
C-H stretch	2278(4)	2270(4)
CH_2 def.	1040(2)	1040(2)
twist	726(2)	726(2)
CH_2 wag	785 720	785 720
CH_2 rock	1011 585	632(2)

[a]Mode assignments are only approximate.
[b]Ref. 52.
[c]This particular value was chosen because it also arises in cyclobutane.

Table XXVI. Out of plane frequencies for the $C_2H_4Cl_2$ and $C_2D_4Cl_2$ activated complexes.

Mode	Nondeuterated complex	Deuterated complex
C-H stretch	3100(3)	2325(3)
CH_2 def	1400(2)	1046(2)
Twist	1000(2)	750(2)
Wag & rock	920(2)	690(2)
C-Cl str. & C-C-Cl rock	700(2)	651(2)
C-Cl bend	400(1)	340(1)

(2). The in-plane-ring vibrational frequencies. Since several bonds are being broken and formed at the same time, the frequencies are difficult to estimate by analogy with known molecules. For this reason a valence-force model with the Wilson F-G matrix method (49) was used to calculate the frequencies. The complexes were treated as four membered rings and the four corners of the ring were treated as point masses. The geometry of the ring was fixed by setting the H-C-C angle equal to the C-C-Cl angle and placing all four corners in the same plane. The internal coordinates were four bond stretches and the bending of the H-C-C valence angle. The procedure was to assign a bond order to the bonds of the complex conserving a bond order of 3. The corresponding bond lengths can be calculated by Pauling's Equation (57). The bending force constant was arbitrarily set at one tenth of the C-H stretching force constant; it mainly affects only the normal mode used as a reaction coordinate. The frequencies taken as the reaction coordinate were very low, on the order of 50 cm^{-1} in all models and closely resembled expected motions of the atoms for HCl elimination reactions (1).

(3). The out of plane ring vibrational frequency. This was treated as an adjustable parameter since there was no precedent to assigning it. It was assigned 400 cm^{-1} for all the nondeuterated complexes. Measured puckering vibrations for small ring molecules are on the order of 200 cm^{-1} or less (67). However, such compounds have carbon, or heavier atoms in the ring and there is no precedent for estimating the frequency of a ring puckering involving an H atoms.

The procedure for the deuterated species was as follows: The Wilson F-G matrix (29) method was used to calculate the ring frequencies for the C_2H_5Cl and C_2D_5Cl 1.8, 0.8, 0.2, 0.2 bond models. At this point the models were treated as four membered rings with appropriate moments of inertia and the Teller-Redlich product rule (53) was used to set the ring puckering for the deuterated ring, keeping the 400 cm^{-1} puckering frequency of the C_2H_5Cl complex constant. Actually the product rule was fit 10% high (deuterated vibrational frequencies were set higher than normal) using the puckering frequency as the variable. Next the out-of-ring frequencies of the complexes were roughly estimated in the same way as for nondeuterated compl eX, i.e., C_2H_4 was used as a model for the C_2H_5Cl complex and C_2D_4 was used as a model for the C_2D_5Cl complex. The entire complex using the calculated ring frequencies, estimated out of ring, and the four atom product rule determined ring puckering was then run through the product rule using the moments of inertia of the total complex including out-of-ring hydrogen coordinates. Minor adjustments were made with the out-of-ring frequencies to bring the product rule agreement to within a 10% (high) fit. This technique was used as the standard for the out of ring C-H frequencies; the other models were constructed by varying the ring frequencies according to the different bond orders (Wilson F-G matric method) and setting the accompanying puckering frequency using the above described product rule procedure for the ring system.

An alternative treatment would be to hold the puckering frequency constant from one model to another and to fit the product

rule by varying the C-H out of ring frequencies. This has the effect of influencing $\Delta\varepsilon_o$ because intermediate value CH_2 bending frequencies must be changed. The former method was used in order to demonstrate the trend believed to be most important. Such changes mark the effect of the ring-frequencies shift upon $\Delta\varepsilon_o$. It was decided to hold the out of ring frequencies constant and fit the product rule by varying the puckering frequency instead. This doesn't affect $\Delta\varepsilon_o$ but does affect the sum ratio more strongly. Thus both procedures have disadvantages.

APPENDIX III
Thermochemistry

In order to calculate RRKM specific rate constants, the critical energy and the energy of the formed molecules must be known. The critical energies were obtained (58) from the Arrhenius activation energies which have been measured in thermal studies. The experimental results are summarized in Table XXVII. The isotopic molecules G_o were calculated by the following equation:

$$\sum_{\text{molecule}}^{3N-6} (1/2h\nu_H - 1/2h\nu_D) - \sum_{\text{complex}}^{3N-7} (1/2h\nu_H - 1/2h\nu_D) + \varepsilon_o(\text{molecule})$$

Since Capon and Ross (16) have verified Tsangs (13) thermal data and also their values are close to Benson's (14) values obtained by a systematic survey of the haloalkanes, these values seem to represent a good average of the known data. With these considerations as a guide, an A factor of $10^{13.5}$ and an E_a of 56.5 kcal $mole^{-1}$ were chosen as the best values. This gives a critical energy of 55.0 kcal $mole^{-1}$.

Table XXVII. Arrhenius parameters.

Molecule	Ref.	Log A (sec^{-1})	G_a (kcal $mole^{-1}$)
C_2H_5Cl	10	14.20	59.50
C_2H_5Cl	11	14.60	60.80
C_2H_5Cl	12	13.51	56.61
C_2H_5Cl	13	13.16	56.46
C_2H_5Cl	14	13.40	57.10
C_2H_5Cl	15	14.03	58.40
C_2H_5Cl	16	13.46	56.62
C_2D_5Cl	18	13.78	58.70

The thermal pyrolysis of 1,2-dichloroethane is complicated by heterogenous effects and radical-sensitized reactions. Thus it was necessary to estimate ε_o for this molecule. A lower limit of 55 kcal $mole^{-1}$ was estimated for ε_o as has been used previously (2).

For a chemical activation system, the chemically activated molecules M* are formed by two radicals R_1 and R_2

$$R_1 + R_2 \dashrightarrow M^*$$

The energy of the activated molecules for such a system may be given by

$$\langle\varepsilon\rangle = \Delta H_f^\circ(M) - H^\circ_f(R_1) - \Delta H^\circ_f(R_2) + \varepsilon_a' + \varepsilon'_{th} = Emin + \varepsilon' th \quad (14)$$

$\Delta H^f_{\circ}$ is the heat of formation at 0 K, ε_a° is the energy of activation of equation 14 and $\varepsilon^\circ th$ is the average thermal energy in the active degrees of freedom of M*. $\varepsilon^\circ th$ is calculated in conjunction with a nonequilibrium distribution function described later. ε_a° has been taken to be 1 kcal $mole^{-1}$ because of previous considerations of CF_3 recombination data (1).

The published values of the pertinent bond dissociation energies disagree and little a priori basis exists for a choice. These values have been surveyed (1,2) and the choices listed in Table XXVIII are those in ref. 1 and 2. Since no new data has been published since then those values will be taken and the reader is referred to these references for a detailed account of the choices.

Table XXVIII. Thermochemistry of radicals[a].

R	D(R-H)	$H_f^o(R)$[b]	$\Delta H_f^o(R-H)$
CH_3	104	35.5	-16.0
CH_2Cl	100	28.7	-18.8
$CHCl_2$	97	25.4	-19.1
CCl_3	95	21.3	-21.3

[a]This table is reproduced from ref. 1 and 2. All values are in kcal $mole^{-1}$

[b]Correct to 0 K $\Delta H_{f(M)}^o$ = 51.6 kcal $mole^{-1}$. Calculated using $\Delta H_f(R) = D(R-H) - \Delta H_f(H) + \Delta H_f(R-H)$

[c]0 K.

Table XXIX. Summary of thermochemical values used.

Molecule	G_a^a	G_o^b	$\Delta H_f^{o\,c}$	Emin[d]
C_2H_5Cl	56.5	55.0	-23.2	88.4
$C_2H_4Cl_2$	e	55[e]	-26.9	85.3

[a]"best" Arrhenius activation energy for the elimination of HCl.

[b]Calculated from ξ_a.(58) Models of complexes are required and the values quoted are average changes for the various models.

[c]0 K.

[d]Equation 14 for definition.

[e]Estimated.

APPENDIX IV
Falloff Calculations

The calculated rate constant for comparison with experiment for thermal systems is

$$\frac{k_{uni}}{k_\infty} = \frac{\int_{\varepsilon_o}^{\infty} \frac{\omega}{k_\varepsilon + \omega} \cdot k_\varepsilon \; k(\varepsilon) \; d\varepsilon}{\int_{\varepsilon_o}^{\infty} k\varepsilon \; \mathcal{K}(\varepsilon) \; d\varepsilon}$$

All terms have been previously defined. Since collision cross sections are temperature dependent, a correction factor was used for the following calculations. Since the collision cross section should be smaller at higher temperatures, Omega integrals (37) were used which are standard factors for correcting temperature dependent transport properties. The Lennard Jones σ value C_2H_5Cl was used for the original cross section and was modified to a final value of 4.5 A. The calculated falloff data for Model II (1.8,.8,.2,.2 bond model) is shown in Table XXXI and fig. 8. The calculated falloff data for Model IIa (deuterated 1.8,.8,.2,.2 bond model) are shown in Table XXXI and fig. 7. The calculated falloff data for C_2H_5Cl appear to fit the experimental values of Heydtmann and Volker (18) well although the experimental falloff do not extend to low pressures. The calculated falloff data in the figures are for 720 K and the values in the table are for 712 K. The $\frac{k_\infty H}{k_\infty D}$ ratio varies less than 5% for the two temperatures. The experimental values of Holbrook and Marsh (15) are seen to fall much faster than either the calculated results or those of Heydtmann. For the deuterated study only the experimental work of Heydtmann and Volker is available for comparison and the experimental values are seen

to fall much faster. Table XXXII shows detailed values at different pressures for the experimental and calculated results. The k_∞ ratio differ by a factor of 25% and this discrepancy was discussed in the text. The agreement between experimental and calculated results become progressively worse as the pressure is lowered. The decrease in isotope effect with pressure has been observed in several experimental studies (methyl isocyanide-d_3 (68) and cyclopropane (69)) and should exist for these chloroethanes. Dr. Heydtmann also questions the reliability of his observed trend with pressure (70).

Table XXX. Comparison of k_∞ at 712 K.

Model	A sec^{-1} [a]	kcal $mole^{-1}$ [a]	(sec^{-1})
Exp	3.25×10^{13} [b]	56.61 [b]	1.17×10^{-4} [c]
Exp_a	6.03×10^{13} [b]	58.70 [b]	5.88×10^{-5}
I	4.03×10^{13}	56.55	2.37×10^{-4}
II	4.03×10^{13}	58.08	9.52×10^{-5}

[a] The comparison is of the form $\frac{Q^+}{Q^*} e^{-E_a/RT}$

[b] Heydtmann and Volker's (18) values taken from Ref. 18.

[c] Heydtmann and Volker's (18) values as given specifically for 712.5 K. The Arrhenius factors will not give this exact value.

[d] 1.8,.8,.2,.2 force bond model.

Table XXXI. Falloff Calculations for C_2H_5Cl and C_2D_5Cl. [a]

C_2H_5Cl		C_2D_5Cl	
Pressure (cm)		Pressure (cm)	
1.0×10^{4}	1.000	1.0×10^{4}	1.000
1.0×10^{3}	1.000	1.0×10^{3}	.999
1.0×10^{2}	.998	1.0×10^{2}	.999
1.0×10^{1}	.981	1.0×10^{1}	.992
1.0×10^{0}	.890	1.0×10^{0}	.994
1.0×10^{-1}	.645	1.0×10^{-1}	.776
1.0×10^{-2}	.324	1.0×10^{-2}	.481
1.0×10^{-3}	.103	1.0×10^{-3}	208
1.0×10^{-4}	.018	1.0×10^{-4}	.063
1.0×10^{-5}	.002	1.0×10^{-5}	.012
1.0×10^{-6}		1.0×10^{-6}	.002

[a] The 1.8,.8,.2,.2 bond models were used for the calculations. The temperature was 712 K.

Table XXXII. Comparison of calculated $\frac{kH}{kD}$ with experimental $\frac{kH}{kD}$ at 712 K.

Pressure (cm)	Experimental[a] $\frac{kH}{kD}$	Calculated[b] $\frac{kH}{kD}$
	1.99	2.49
.61	1.95	2.26
.51	2.20	2.24
.44	2.17	2.23
.24	2.30	2.20
.10	2.56	2.01
.063	2.44	1.96
.022	2.71	1.81
1.0×10^{-2}		1.63
1.0×10^{-3}		1.20
4.7×10^{-4}		1.00
1.0×10^{-4}		.68

[a] Heydtmann and Volkers's (18) experimental values were used.

[b] Calculated using model II; the 1.8, .8, .2, .2 bond model.

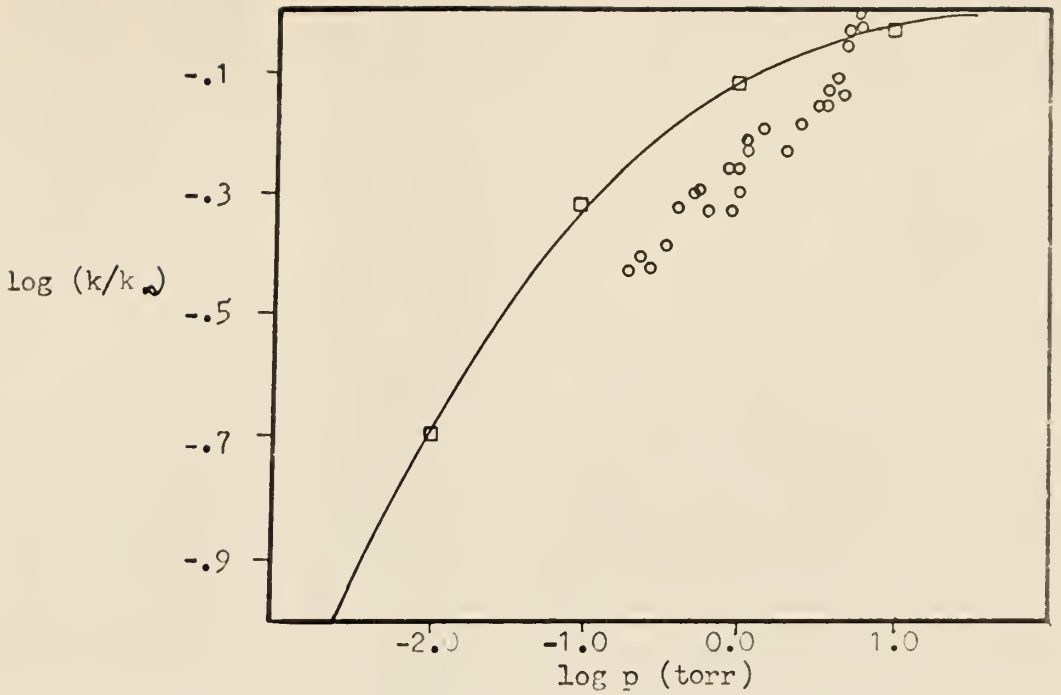

Fig. 7. Comparison of calculated and experimental falloff data for C_2D_5Cl. □ = calculated values at 720 K; ○ = experimental values of Heydtmann and Volker (ref. 18) at 712.5 K.

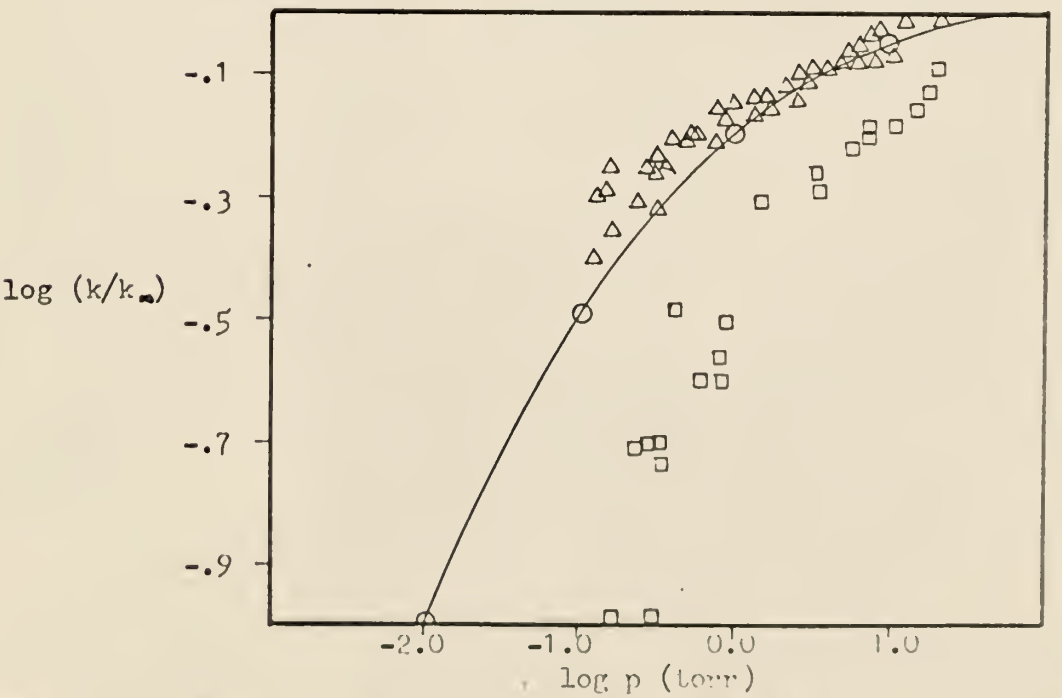

Fig. 8. Comparison of calculated and experimental falloff data for C_2H_5Cl. ○ = calculated values at 720 K; △ = experimental values of Heydtmann and Volker (ref. 18) at 712.5 K; □ = experimental values of Holbrook and Marsh (ref. 15) at 730 K.

APPENDIX V

$1,1\text{-}C_2H_4Cl_2$

This appendix contains revised calculations of $1,1\text{-}C_2H_4Cl_2$ (1,2) using an asymmetric 1.8,.8,.2,.2 bond model complex found to be favorable in this thesis.

The frequencies of the molecule are known (71) and are as follows(geometrically grouped): 2953(4), 1356(5), 1044(3), 677(2), 358(2), and 257(2). Since $1,1\text{-}C_2H_4Cl_2$ and $1,2\text{-}C_2H_4Cl_2$ lead to the same decomposition products the same out of ring frequencies were used and are as follows: 3100(3), 1400(2), 920(2), 700(2), 400(1). Using a 1.8,.8,.2,.2 bond model and Pauling's (57) form of Badger's rule to obtain the stretching force constants the usual Wilson F-G matrix calculation yielded the following in ring frequencies: 946, 403, 919, 853, and 33, where 33 was taken as the reaction coordinate. The total geometrically grouped frequencies for the complex were then 3100(3), 1400(2), 1000(2), 926(4), 748(3), and 401(3).

The moments of inertia for the molecule and complex were calculated on a 1410 computer using literature (71,72) parameters for the molecules and parameters for the complex which consisted of a 1.8,.8,.2,.2 bond model with a α H atom of the out of ring C-H replaced by a Cl atom and extended to the C-Cl length. The calculated moments of inertia were

molecule moments of inertia, a.m.u.	complex moments of inertia, a.m.u.
80.80	78.09
160.3	140.8
226.0	218.7

The rate constants were calculated using previous (12) thermal data (ε_o = 52 kcal mole^{-1}, Emin = 88.4 kcal mole^{-1}) and are tabulated in Table XXXIII.

Table XXXIII. 1,1-$C_2H_4Cl_2$ rate constants.

Model	A[a] (sec^{-1}) 800 K	k_a (sec^{-1}) 298 K
Exp[ab]	1.24×10^{13}	1.10×10^{10}
1.8,.8,	1.96×10^{13}[c]	
.2,.2		3.86×10^{9}

[a] A factor given by $kT/h\ Q^{\ddagger}/Q^*$
[b] Ref 1 and 2
[c] Corrected for internal rotation by a factor of .78. This factor was calculated using a method due to Wilson (73).

The original calculation (1,2) contained an error in the complex moments of inertia due to a systematic error in evaluation of the coordinates of the out-of-ring atoms. The new evaluation decreased the rotational partition function ratio a factor of about 40%. Also the C-H stretches were raised from 2933(3) to 3100(3), the intermediate frequencies lowered somewhat and the C-Cl bend raised from 300 to 400 cm^{-1}. The puckering frequency was lowered from 500 cm^{-1} to 400 cm^{-1}. The total effect was a 29% lowering of the thermal A factor and a $\approx$ 20% lowering of k_a from the original calculations; the lower rotational partition function ratio and generally higher intermediate frequencies being counterbalanced by the lower puckering frequency.

ACKNOWLEDGMENTS

The author wishes to gratefully acknowledge his major professor, Dr. D. W. Setser for guidance and encouragement throughout the performance of this work.

Grateful acknowledgment is extended to Dr. H. Heydtmann for initiating correspondence and supplying a valuable manuscript on the thermal pyrolysis of chloroethane-d_0 and d_6 used extensively as a reference throughout this thesis. Particular thanks are also due R. L. Johnson for many helpful discussions of the theory.

Support of this work by the National Science Foundation is gratefully acknowledged.

LITERATURE CITED

1. J. C. Hassler, Ph.D. thesis, Kansas State University, 1966.
2. J. C. Hassler and D. W. Setser, J. Chem. Phys., 45, 3246 (1966).
3. R. L. Johnson and D. W. Setser, submitted to J. Phys. Chem., May, 1967.
4. R. A. Marcus and O. K. Rice, J. Phys. & Colloid Chem., 55, 894 (1951).
5. R. A. Marcus, J. Chem. Phys. 20, 352, 359 (1952).
6. R. A. Marcus, J. Chem. Phys., 43, 2658 (1965).
7. G. H. Kohlmaier and B. S. Rabinovitch, J. Chem. Phys., 38, 1692 (1963). A descriptive application is given.
8. D. W. Setser, R. Littrell, and J. C. Hassler, J. Am. Chem. Soc., 87, 2062 (1965).
9. J. C. Hassler, D. W. Setser, and R. L. Johnson, J. Chem. Phys, 45, 3231 (1966).
10. D. H. R. Barton and K. E. Howlett, J. Chem. Soc., 1949 155, 165.
11. K. E. Howlett, J. Chem. Soc., 1952, 3695, 4487.
12. H. Hartmann, H. G. Bosche, and H. Heydtmann, Z.Physik. Chem. (Frankfurt), 42, 329 (1964).
13. W. Tsang, J. Chem. Phys., 41, 2487 (1964). This author cites and summarizes many earlier data on alkyl halide eliminations.
14. S. W. Benson and A. N. Bose, J. Chem. Phys. 39, 3463 (1963).
15. K. A. Holbrook and A. R. W. Marsh, Trans. Far. Soc., 63, 643, (1967).
16. N. Capon and R. A. Ross, Trans. Faraday Soc., 62, 1560 (1966).
17. A. T. Blades, P. W. Gilderson, and M. G. H. Wallbridge, Can J. Chem., 40, 1526 (1962).
18. H. Heydtmann and C. W. Volker, Zeitschrift fur Physikalishe Chemie (Frankfurt), 55, 296 (1967).
19. J. W. Simons, B. S. Rabinovitch, and R. F. Kubin, J. Chem Phys., 40, 3343 (1964).
20. B. S. Rabinovitch and J. H. Current, Can. J. Chem., 40, 557 (1962)
21. J. H. Current and B. S. Rabinovitch, J. Chem. Phys., 38, 1967 (1963).
22. J. H. Current and B. S. Rabinovitch, J. Chem. Phys., 38, 783, (1963).
23. B. S. Rabinovitch and D. W. Setser, J. Am. Chem. Soc., 84, 1765 (1962).
24. J. W. Simons, and D. W. Setser, and B. S. Rabinovitch, J. Am Chem. Soc., 84, 1758 (1962).
25. W. E. Falconer, B. S. Rabinovitch, and R. J. Cvetanovic, J. Chem. Phys., 39, 40 (1963).
26. J. W. Simons and B. S. Rabinovitch, J. Phys. Chem., 68, 1322 (1964).
27. D. W. Setser, J. Phys. Chem., 70, 826 (1966).
28. D. W. Setser and J. C. Hassler, J. Phys. Chem., 71, 1364 (1967).
29. A. W. Read, Progr. Reaction Kinetics, 3, 203 (1965).

30. W. A. Noyes, Jr., and P. A. Leighton, "Photochemistry of Gases," Reinhold Publ. Corp., New York, N.Y., 1944.
31. Available form Electronics Space Products, Inc.
32. J. A. Kerr and A. F. Trotman, Progr. Reaction Kinetics, 1, 105 (1961).
33. W. G. Alcock and E. Whittle, Trans. Faraday Soc., 61, 244 (1965).
34. B. S. Rabinovitch and D. W. Setser, Advan. Photochem., 3, 53 (1964).
35. B. S. Rabinovitch and R. W. Diesen, J. Chem. Phys., 30, 735 (1959).
36. D. W. Setser, B. S. Rabinovitch, and J. W. Simons, J. Chem. Phys., 40, 1751 (1964).
37. J. O. Hirschfelder, C. F. Curtiss, and R. B. Bird, "Molecular Theory of Gases and Liquids," John Wiley and Sons, Inc., New York, N. Y., 1954.
38. B. S. Rabinovitch and D. W. Setser, Advan. Photochem., 3, 42 (1964).
39. R. S. B. Johnstone and R. P. Wayne, Photochemistry and Photobiology, 6, 531 (1967).
40. Terry E. Sharp and Harold S. Johnstone, J. Chem. Phys., 37, 1541 (1962).
41. A. T. Blades, Can. J. Chem. 39, 1401 (1961).
42. J. Langrish and H. O. Pritchard, J. Phys. Chem., 761 (1958).
43. A. T. Blades, Can. J. Chem., 36, 1043 (1958).
44. A. T. Blades, P. W. Gilderson and M. G. H. Wallbridge, Can. J. Chem., 40, 1533 (1962).
45. J. W. Simons, B. S. Rabinovitch, and D. W. Setser, J. Chem. Phys., 41, 800 (1964).
46. G. H. Kohlmaier, and B. S. Rabinovitch, J. Chem. Phys., 38, 1709 (1963).
47. H. S. Johnston and P. Goldfinger, J. Chem. Phys., 37, 700 (1962).
48. W. L. S. Andrew and George C. Pimentel, J. Chem. Phys., 44, 2527 (1966).
49. E. B. Wilson, J. C. Decius, and P. C. Cross, "Molecular Vibrations," McGraw-Hill Book Co., Inc., New York, N. Y., 1955.
50. Norman Davidson, "Statistical Mechanics," McGraw-Hill Book Company, Inc., New York, N. Y., 102 (1962).
51. J. H. S. Green and D. J. Holden, J. Chem. Soc., 1962, 1794.
52. I. Nakagawa and S. Mizushima, J. Chem. Phys., 21, 2195 (1953).
53. Kenneth S. Pitzer, "Quantum Chemistry," Prentice-Hall, Inc., Englewood Cliffs, N. J., 492 (1960).
54. J. E. Piercy, J. Chem. Phys., 43, 4066 (1965).
55. R. H. Schwendermann and C. D. Jacobs, J. Chem. Phys., 36, 1245 (1962).
56. B. N. Cyvin and S. J. Cyvin, Acta Chemica Scandinavia, 17, 1831 (1963).
57. L. Pauling, "The nature of the Chemical Bond," 3rd ed., Cornell University Press, Ithaca, N. Y., 1960.
58. S. Glasstone, K. J. Laidler, and H. Eyring, "The Theory of Rate Processes," McGraw-Hill Book Co., New York, N.Y., 194 (1962).

59. S. W. Benson and G. R. Haugen, J. Am. Chem. Soc., 87, 4036 (1965).
60. H. S. Johnston, "Gas Phase Reaction Rate Theory", Ronald Press Company, New York, N. Y., (1966).
61. R. M. Badger, J. Chem. Phys., 2, 128 (1934).
62. D. R. Herschbach and V. W. Laurie, J. Chem. Phys., 35, 458 (1961).
63. H. S. Johnston, J. Am. Chem. Soc., 86, 1643 (1964).
64. K. D. Moller and L. H. London, J. Chem. Phys., 47, 2505 (1967).
65. P. C. Haarhoff, J. Mol. Phys., 6, 337 (1963).
66. H. M. Frey and G. B. Kistiokowsky, J. Am. Chem. Soc., 79, 6373 (1957).
67. For example see James R. Durig, W. H. Green and N. C. Hammond, J.Phys. Chem., 70, 1989, (1966).
68. F. W. Schneider and B. S. Rabinovitch, J. Am. Chem. Soc., 85, 2365 (1963).
69. B. S. Rabinovitch, P. W. Gilderson, and A. T. Blades, J. Am. Chem. Soc., 86, 2994 (1963).
70. Private communication with Dr. H. Heydtmann.
71. M. D. Danford and R. L. Livingston, J. Am. Chem. Soc., 81, 4157 (1959).
72. L. W. Daasch, C. Y. Learing, and J. R. Nielsen, J. Chem. Phys., 22, 1293 (1954).
73. E. B. Wilson, Chem. Rev., 27 17 (1940).

NONEQUILIBRIUM ISOTOPE EFFECTS IN THE UNIMOLECULAR REACTIONS OF CHEMICALLY ACTIVATED CHLOROETHANES

by

KENNETH DEES

B. S., Utah State University, 1965

AN ABSTRACT OF A MASTER'S THESIS

submitted in partial fulfillment

of the requirements for the degree

MASTER OF SCIENCE

Department of Chemistry

KANSAS STATE UNIVERSITY
Manhattan, Kansas

1968

ABSTRACT

The HCl elimination reactions from C_2H_5Cl and 1,2-$C_2H_4Cl_2$ proceed by a four-centered activated complex. Such transition states are not well understood and isotope effects are a possible tool for gaining further understanding of their nature. A gas phase chemical activation technique was employed for the production of the molecules. CH_2 and CD_2 formed by photolysis of the appropriate ketene were allowed to undergo abstraction reactions with CH_3Cl and CD_3Cl, respectively. Highly vibrationally excited C_2H_5Cl, C_2D_5Cl, $C_2H_4Cl_2$ and $C_2D_4Cl_2$ molecules were generated by the recombination of the resulting CH_3 and CH_2Cl or CD_3 and CD_2Cl radicals. These chloroethanes then undergo unimolecular elimination of HCl or DCl to the corresponding olefin. The nonequilibrium unimolecular elimination rate constants were measured as follows at an energy of ~ 90 kcal mole^{-1}. C_2H_5Cl, 4.6×10^9 sec^{-1}; C_2D_5Cl, 1.4×10^9 sec^{-1}, 1,1-$C_2H_4Cl_2$, 2.0×10^8 sec^{-1}; and 1,2-$C_2D_4Cl_2$, 5.7×10^8 sec^{-1}. The resulting $\frac{k_{aH}}{k_{aD}}$ are 3.3 ± .4 and 3.5 ± .1 for the chloroethanes and 1,2-dichloroethanes, respectively.

The data were interpreted according to the RRKM (Rice-Ramsperger-Kassel-Marcus) theory of unimolecular reactions. Several transition state models for chloroethane, identified by different bond orders of the bonds in the planar four-centered complex, were studied. It proved possible to fit both the nonequilibrium data and also thermal equilibrium kinetic data available from the literature. The overall kinetic data appears to favor the asymmetric bond models rather than a symmetric bond model. For the case of

1,2-dichloroethane, the lack of Arrhenius parameters prohibited making a detailed study of the different transition state models.

In an effort to learn whether or not deactivation probabilities exhibit an isotope effect, a "stepladder" deactivation model was used to evaluate the behavior of k_a at the low pressure region where the effects of inefficient collisional deactivation can be observed. Essentially, this model assumes that a constant quantity of energy, called a "stepsize" is removed from the excited molecule by each collision. The probabilities were measured by comparing the competition between unimolecular reaction and collisional deactivation at the low pressures. The calculations were carried out for C_2H_5Cl, C_2D_5Cl, $C_2H_4Cl_2$, and $C_2D_4Cl_2$ using CH_3Cl and CD_3Cl as the deactivating molecules for the nondeuterated and deuterated species, respectively. It was found that within experimental error no isotope effect was exhibited. The chloroethanes lose $\approx$ 12-14 kcal $mole^{-1}$ per collision with the CH_3Cl and CD_3Cl molecules.